Journal of Drug Delivery Science and Technology 115 (2026) 107628

Contents lists available at ScienceDirect

Journal of Drug Delivery Science and Technology

journal homepage: www.elsevier.com/locate/jddst

Electrospun fibers loaded with extracts of *Gunnera tinctoria* and *Buddleja globosa* with potential application in the treatment of skin lesions

Jeyson Hermosilla [a,b,c,d], Cátia Alves [e], Andrea Zille [e], Jorge Padrão [e], Claudia Sanhueza [f,g], Edgar Pastene-Navarrete [h,i], Francisca Acevedo [b,c,d,j,*]

[a] Programa de Doctorado en Ciencias de Recursos Naturales, Universidad de La Frontera, Avenida Francisco Salazar 01145, Casilla 54-D, Temuco, 4780000, Chile
[b] Center of Excellence in Translational Medicine (CEMT), Facultad de Medicina, Universidad de La Frontera, Avenida Alemania 0458, Temuco, Chile
[c] Scientific and Technological Bioresource Nucleus (BIOREN), Universidad de La Frontera, Avenida Francisco Salazar 01145, Casilla 54-D, Temuco, Chile
[d] Millennium Nucleus Bioproducts, Genomics and Environmental Microbiology (BioGEM), Avenida España 1680, 2390123, Valparaíso, Chile
[e] Centre for Textile Science and Technology (2C2T), Azurém Campus, University of Minho, 4800-058, Guimarães, Portugal
[f] Center for Resilience, Adaptation and Mitigation (CReAM), Universidad Mayor, Avenida Alemania 0281, Temuco, Chile
[g] Escuela de Ingenieria, Facultad de Ciencias, Ingenieria y Tecnologia, Universidad Mayor, Avenida Alemania 0281, Temuco, Chile
[h] Laboratorio de Síntesis y Biotransformación de Productos Naturales, Universidad del Bío-Bío, Avda. Andrés Bello 720, Chillán, Chile
[i] Laboratorio de Farmacognosia, Departamento de Farmacia, Facultad de Farmacia, Universidad de Concepción, Barrio Universitario S/N, PO Postal 237, Concepción, Bío Bío, Chile
[j] Department of Basic Sciences, Faculty of Medicine, Universidad de La Frontera, Avenida Francisco Salazar 01145, Casilla 54-D, Temuco, Chile

ARTICLE INFO

Keywords:
Encapsulation
Wound dressing
Chronic wound
Electrospinning
Gunnera tinctoria
Buddleja globosa

ABSTRACT

This study reports the development of electrospun polycaprolactone (PCL) fibers loaded with bioactive extracts of *Gunnera tinctoria* and *Buddleja globosa* for potential applications in wound healing. Plant extracts were obtained using green extraction methods (aqueous and hydroalcoholic) and characterized via FTIR, HPLC, and antioxidant assays. The *G. tinctoria* extract exhibited the highest total polyphenol content and antioxidant activity, correlating with enhanced biological performance in fiber formulations. Among the formulations evaluated, the formulation composed of 1 mg/mL of *G. tinctoria* and *B. globosa* extracts incorporated into a 14 % (w/v) PCL matrix (referred to as formulation P4) demonstrated the most favorable combination of morphological uniformity, cytocompatibility, and antifungal activity. FTIR analysis of the fibers confirmed characteristic PCL signals, while signals corresponding to the encapsulated extracts were not clearly distinguishable, likely due to their internal incorporation within the polymer matrix. *In vitro* antimicrobial assays did not display antibacterial activity against *Staphylococcus aureus* and *Pseudomonas aeruginosa*. Nonetheless, a significant antifungal effect was observed in P4 against *Candida albicans* of log reduction 4.1, thus being classified as a moderate disinfectant. Cell viability assays using 3T3-L1 fibroblasts showed excellent biocompatibility for extract-loaded fibers, particularly those containing *G. tinctoria*, with P4 maintaining high viability after 72 h. These findings support the potential of bioactive PCL fibers as advanced wound dressing materials. Further studies are recommended to optimize extract loading, evaluate controlled release profiles, and validate efficacy in *in vivo* wound healing models.

1. Introduction

The skin is highly susceptible to various types of injuries, broadly classified as acute wounds resulting from burns, trauma, abrasions or chronic wounds, such as those seen in cases like diabetic foot ulcers [1]. Skin lesions are prone to infections caused by a variety of microorganisms, including Gram-positive bacteria such as *Enterococcus* sp., *Staphylococcus aureus* (known to cause numerous skin infections), and *Bacillus thuringiensis*. Moreover, Gram-negative bacteria such as *Pseudomonas aeruginosa*, *Escherichia coli*, *Enterobacter* sp., or *Klebsiella pneumoniae*,

* Corresponding author. Center of Excellence in Translational Medicine (CEMT), Facultad de Medicina, Universidad de La Frontera, Avenida Alemania 0458, Temuco, Chile.
E-mail addresses: j.hermosilla03@ufromail.cl (J. Hermosilla), catia.alves@2c2t.uminho.pt (C. Alves), azille@2c2t.uminho.pt (A. Zille), padraoj@2c2t.uminho.pt (J. Padrão), claudia.sanhuezas@umayor.cl (C. Sanhueza), epastene@ubiobio.cl (E. Pastene-Navarrete), francisca.acevedo@ufrontera.cl (F. Acevedo).

https://doi.org/10.1016/j.jddst.2025.107628
Received 17 July 2025; Received in revised form 3 October 2025; Accepted 5 October 2025
Available online 6 October 2025

fungi such as *Candida* spp., and viruses such as herpes simplex virus, cytomegalovirus, or varicella-zoster virus, pose other threats [2–4]. The severity of microbial infections stems from a combination of factors, such as: the ability to colonize the lesion (adhesion to host cells and tissues), expression of proteolytic enzymes, capacity to harvest nutrients from the host, and evasion of the patient's immune system. The prevalence of microbial infections and their associated complications is increasing, primarily due to the escalating resistance to antimicrobial drugs used in conventional or widely practiced treatments [5]. Therefore, there is an urgent need for effective alternatives to combat these infections, such as angiogenesis regulators, calcium channel blockers, or phytochemicals [6]. Plants produce diverse bioactive compounds that have found extensive application in clinical practice. Many of these compounds derived from plants are safer due to their natural origin than synthetic counterparts [7]. There is a growing interest in utilizing crude extracts from medicinal plants and screening plant-derived compounds as potential alternative therapies for microbial infections [8]. Traditional knowledge from indigenous cultures and recent scientific research attribute diverse therapeutic properties to *Gunnera tinctoria* and *Buddleja globosa*, particularly emphasizing their healing, antimicrobial, and antioxidant properties. *G. tinctoria*, a large-leafed herbaceous plant endemic to southern Chile and Argentina, has been utilized for medicinal, dyeing, and culinary purposes. In Mapuche traditional medicine, its leaves have been used topically to treat wounds, burns, and ulcers due to their antiseptic and anti-inflammatory effects. Phytochemical analyses have identified this species as a rich source of bioactive phenolic compounds, including ellagic acid, gallic acid, chlorogenic acid, and various hydrolyzable tannins, which are strongly associated with its high antioxidant capacity and antimicrobial efficacy. Studies have demonstrated that aqueous and hydroalcoholic extracts of *G. tinctoria* inhibit the growth of *Listeria monocytogenes*, *S. aureus*, *E. coli*, and *P. aeruginosa*, although Gram-negative strains tend to show greater resistance due to their outer membrane complexity [9–12]. These properties underscore the potential of *G. tinctoria* for applications in the nutraceutical, cosmetic, and biomedical fields, particularly for the design of functional materials for wound care. *B. globosa*, commonly known as matico, is a woody evergreen shrub native to the Andean regions of Chile, Argentina, Peru, and Bolivia. Its leaves and stems have been traditionally employed for centuries in the treatment of skin lesions, inflammation, and pain, as well as for respiratory and gastrointestinal disorders. Chemical characterization of *B. globosa* has revealed a diverse profile of pharmacologically active constituents, including flavonoids (e.g., luteolin, diosmetin), phenylethanoids (e.g., verbascoside, forsythoside B), phytosterols, and triterpenoids. These compounds have been associated with the plant's antioxidant, anti-inflammatory, and wound healing properties [13–16]. *In vivo* studies in murine models have demonstrated that *B. globosa* leaf extracts accelerate wound closure, promote reepithelialization, and modulate inflammatory responses by reducing proinflammatory cytokine levels (e.g., TNF-α, IL-1β, and IL-6) and oxidative stress markers [17]. Antinociceptive effects have also been attributed to specific phenolic constituents, supporting its traditional use for pain relief [15,18]. Moreover, cytotoxicity studies have shown low toxicity levels of *B. globosa* extracts on human fibroblast and keratinocyte cultures, further supporting their safe use in dermal applications.

Electrospinning stands out as the most versatile and effective technique for producing ultrafine micro- and nanofibers, which can be loaded with bioactive compounds [19,20]. Unlike other approaches, electrospinning allows precise control of fiber morphology and enables the fabrication of structures with high surface-to-volume ratios, interconnected porosity, and tunable architectures (e.g., porous, core–shell, or aligned). These features are particularly advantageous for wound healing applications, as they promote efficient exudate absorption, water management, and the creation of a moist microenvironment conducive to tissue regeneration. Moreover, electrospun fibers act as adaptive, non-adherent physical barriers with a large surface area capable of accommodating and releasing active agents in a controlled manner [21]. Compared with recently developed alternatives, such as pressurized spinning systems designed for sustainability [22], electrospinning remains superior in versatility, as it does not rely exclusively on aqueous solutions and can process highly hydrophobic polymers such as polycaprolactone (PCL), widely used in biomedical research. Although pressurized spinning reduces solvent use and energy consumption, its application is limited when polymers require organic solvents (e.g., chloroform for PCL), making electrospinning the most suitable and reliable technique for developing functional nanofiber dressings. Recent studies reinforce this advantage by proposing composite electrospun membranes with antimicrobial agents, such as silver nanoparticles or drug-loaded fibers, highlighting their capacity to accelerate burn healing and wound regeneration [23]. Over the past decade, investigations have explored the production of burns and wounds dressings using fibers loaded with plant extracts, harnessing their numerous beneficial effects. Several components and secondary metabolites of plant origin have demonstrated promising agents for wound and burn treatment due to their lower toxicity and potent healing and antioxidant properties. Published studies [24–26] have indicated that natural extracts incorporated into electrospinning exhibit antimicrobial effects or can support healing wounds and burns. In addition, polycaprolactone (PCL) fibers exhibit several properties that make them particularly suitable for tissue regeneration. These properties include their extracellular matrix-like morphology, biocompatibility, surface tunability, and potential for incorporating bioactive agents, which promote cell adhesion, proliferation, and differentiation [27–30]. Furthermore, the envisaged objective of this research is to develop electrospun fibers based on the electrospinning method, using PCL as the polymer matrix, and incorporating bioactive compounds from natural extracts of *G. tinctoria* and *B. globosa*. These fibers aim to possess physical, chemical, and biological properties promoting antimicrobial activity and cellular proliferation.

2. Materials & methods

2.1. Materials

The lyophilized extract of *G. tinctoria* was provided by Dr. Edgar Pastene from Universidad del Bio-Bio, Chillán, Chile. The plants were purchased at the Municipal Market of Concepción, Chile. In addition, these plants were classified and deposited in the herbarium of the Faculty of Pharmacy at of the Andrés Bello University. The extracts were obtained through an aqueous extraction process involving the petioles mechanical liquefaction (their edible section), filtration and centrifugation. The aqueous extracts were adsorbed on columns packed with Sepabeads SP-850 preconditioned with water. To remove sugars, salts and proteins, the column was washed with distilled water, then the adsorbed compounds were recovered with ethanol 95 % (v/v). The ethanolic extract was concentrated under a vacuum and finally freeze-dried. The total extract of *G. tinctoria* (denominated "N") was stored at −20 °C until use [9]. The leaves of *B. globosa* were collected in semirural sectors between the communes of Cunco and Freire, La Araucanía Region, Chile. Season collections were performed, one in winter and the other in spring. The herbalization of a sample of the collected plant material was carried out according to the manual "Confection of a CONC herbarium". The voucher specimen was deposited in this certified CONC herbarium. The leaves were washed with distilled water and air-dried at room temperature, and the damaged parts were removed. Aqueous and hydroalcoholic extracts were developed; in both cases, a ratio of 20 g of plant material in 500 mL of water or with ethanol/water 50 % (v/v) was used. The solution was stirred for 24 h at room temperature. Finally, the process was aided with 30 min of ultrasound to increase the extraction yield. The ethanol from the hydroalcoholic extracts was removed using a vacuum concentrator (Eppendorf Concentrator plus, Germany). Subsequently, the samples were frozen at −80 °C and freeze-dried at 1 Pa pressure and −80 °C in a freeze dryer BK-FD18P (Biobased Group,

China). The lyophilized extract was stored in a desiccator until later use.

2.2. Electrospinning procedure

The electrospun fibers were developed using an electrospinning unit (NEU-BM, China) and adjusting the parameters to those previously published by our team [31], with the aim of obtaining a stable flow and continuous, defect-free fibers. The flow of the polymer solution was regulated by a syringe pump, which applied a controlled pressure to ensure a constant flow from the capillary outlet. The prepared solutions were loaded into 10 mL plastic syringes, connected with #8 needles (inner diameter of 0.4 mm and 25 mm length). Electrospinning experiments were conducted under ambient conditions (25 °C and 50 % relative humidity), and the fibers were collected on a rotating drum (50 rpm) covered with aluminum foil. Polycaprolactone (PCL) 80.000 average M_n (Sigma-Aldrich, Germany) solutions were prepared using chloroform as the solvent. The distance between the needle and the collector was set at 20 cm, with voltages of 0 and 25 kV. Various concentrations (0.1, 0.5, and 1.0 mg/mL) of *G. tinctoria* and *B. globosa* extracts incorporated into the fibers were evaluated.

2.3. Scanning electron microscopy

The fiber diameter (Y_d) and the morphology index (Y_m) were determined using images obtained by scanning electron microscopy (SEM). A STEM SU-3500 variable pressure scanning electron microscope (SEM) (Hitachi, Japan) was used. Images from each experimental point were used at the same magnification level and 100 different segments were measured randomly using the public domain software ImageJ (National Institute of Health, USA). The results were expressed as the mean ± standard deviation. The value of the morphology index (Y_m) was calculated by means of a qualitative evaluation based on the characteristics of the fibers [32]. The first step was to assign a value of (1) to the presence of unwanted artifacts in the samples, such as pearls, agglomerations, and spheres. The SEM images of the fibers were divided into 20 equal portions. If at least one of these unwanted artifacts is observed in the analyzed portion, the value of (1) will be assigned, otherwise the value of (0) will be assigned. To calculate the morphology index (Y_m), equation (1) (Eq. (1)) was used. With this protocol, when the defects are not very prominent, the index is closer to the value 1.

$$Y_m = 1\text{-}\left(\sum \text{portions value} \Big/ 20\right) \quad \text{Eq. (1)}$$

2.4. Tensile test

Mechanical properties were measured using CT3 Texture Analyzer (Brookfield Engineering Labs. Inc., USA). For tensile testing, the sample with 60 × 10 × 0.2 mm in size was held between two sets of rollers, and the system recorded the force and displacement until the sample peeled off at a rate of 30 mm/min. The thickness of the test samples was measured using a digital micrometer. The Young's moduli (E) of the samples were calculated from the Hooke's region of the tensile traces. These assays were performed in triplicate.

2.5. FTIR analysis

The chemical structures were determined by attenuated total reflection Fourier transform infrared (ATR-FTIR), where a FTIR-4600 was used (JASCO Co., Japan). A scanning range of 4500–600 cm^{-1} was used, with a resolution of 4 cm^{-1}, 20 scan for sample. All results were expressed as percentage transmittance (%T).

2.6. High-performance liquid chromatography (HPLC) analysis

Identification was performed by HPLC–DAD-ESI/MS. The ESI-MS system consisted of a YL 9100 chromatograph (Young Lin Instrument Co. Ltd., South Korea), controlled by the YL-Clarity MS Extension software. To determine the phenolic compounds in the extracts obtained, the extracts were analyzed at UV 270 and 330 nm. The methodology was based on [17] with slight modifications.

2.7. Polyphenol content

The total content of polyphenols in the extracts was determined using the method described by Ref. [33] with modifications, using the Folin-Ciocalteu reagent (Sigma-Aldrich, Germany) and molecular spectrophotometry at 740 nm. Briefly, 50 μL of each point of the gallic acid (ChemCruz, Santa Cruz Biotechnology, USA) calibration curve was added in triplicate into a 96-weel plate, followed by the addition of 200 μL of aqueous solution of Folin-Ciocalteu 10 % (v/v) and 50 μL of sodium carbonate at 5 % (w/v). For the samples, the gallic acid standard was replaced by 50 μL of the diluted plant extract (three dilution factors were applied per sample in triplicate). Subsequently, the 96-well plate was incubated at 37 °C in an oven for 20 min. Finally, the absorbance was measured using a microplate reader at 740 nm. The results were expressed as equivalent milligrams of gallic acid per grams of dry extract (mg GAEq/g dry extract).

2.8. Thermal analysis

The electrospun fibers were analyzed by thermogravimetry (TGA) and differential scanning calorimetry (DSC) to determine their thermal behavior using DSC equipment, STA 6000 (PerkinElmer, USA), under a nitrogen atmosphere (40 mL/min). The analyses were recorded from 25 to 600 °C at a heating rate of 15 °C/min.

2.9. In vitro antioxidant activity

The antioxidant activity was assessed by the ability of the samples to reduce the 2,2-diphenyl-1-picrylhydrazyl free radical DPPH (ChemCruz, Santa Cruz Biotechnology, USA), which was measured using the method of Brand-Williams et al. [34] modifying gallic acid with Trolox (ChemCruz, Santa Cruz Biotechnology, USA). Briefly, measurements were made at an absorbance of 517 nm in a BioRad model 680 UV microplate reader (BioRad Laboratories, Inc., USA) in triplicate. The calibration curve was carried out with Trolox (0–800 μM). The antioxidant capacity of each sample was expressed as mg equivalent of Trolox per milligram of dry extract (mg TroloxEq/mg dry extract).

2.10. In vitro antimicrobial activity

Semi-quantitative analysis of natural extracts was performed through the minimum inhibitory concentration (MIC), half minimum bactericidal concentration (MBC_{50}), and half minimum fungicidal concentration (MFC_{50}), using an adaptation of the standard Clinical and Laboratory Standards Institute (CLSI) and the European Committee on Antimicrobial Susceptibility Testing (EUCAST), a microdilution method described by Ref. [35]. A quantitative antimicrobial analysis was also performed according to American Association of Textile Chemists and Colorists (AATCC) test method 100-TM100. These methodologies are routinely performed in the Host Research Centre [36–38].

2.10.1. Minimum inhibitory concentrations (MIC) and minimum bactericidal/fungicidal Concentration50 (MBC/MFC)

MICs were determined using the broth microdilution procedure [39] against *S. aureus*, *P. aeruginosa*, and *C. albicans*. The working solutions were prepared 4 mg for each natural extract (N, M1, M2, M3, and M4) with 2 mL of distilled water. Serial dilutions (1:10) were made with distilled water in the consecutive wells, to a final volume of 100 μL (2.000, 1.000, 0.500, 0.250, 0.125, 0.063, 0.031 and 0.016 mg/mL). Then, 100 μL of the microorganisms' suspensions prepared at 2.0 × 10^5

colony forming unit (CFU)/mL in Mueller Hinton broth (MHB, Liofilchem, Terano, Italy) were added to each of these wells (using three replicates). Extract-free microorganism suspensions in distilled water were used as negative control and the microorganism suspensions at a final concentration of 1.0×10^7 CFU/mL were used as a positive control. Optical density (OD) at a wavelength of 600 nm (bacteria) and 640 nm (fungi) was measured in a EZ READ 2000 Microplate Reader (Biochrom, UK) before and after plate incubation for 20 h, at 120 rpm of shaking speed, at 37 °C (bacteria) or 30 °C (fungi). The MIC value for each extract/bacteria combination was established as the concentration at which bacteria were determined visually, and confirmed by the differences in OD. OD were calculated using equation (2) (Eq. (2)):

$$OD = OD_{T_{20}} - OD_{T_0} \quad \text{Eq. (2)}$$

were, $OD_{T_{20}}$ is the absorbance at 20 h of incubation, and OD_{T_0} is the absorbance at time zero.

Once the MIC was determined for each extract, the MBC and MFC were identified by analyzing variations in absorbance values, following the methodology presented in Ref. [40]. Subsequently, aliquots of the bacterial/fungal dispersion, selected based on the MIC, were collected, serially diluted in phosphate buffer saline (PBS), and plated on tryptic soy agar Petri dishes. After incubation at 37 °C for 16 h, the colonies were counted, and the MBC/MFC values were determined.

2.10.2. Test method 100-TM100

The antimicrobial activity of electrospun fibers was performed using the AATCC test method 100-TM100 (contact killing) (AATCC, 2012) with slight modifications as described in Ref. [41]. This methodology was adapted for electrospun fibers loaded with natural extracts, evaluated against *S. aureus*, *P. aeruginosa* and *C. albicans*. Briefly, fibers with 16 mm of diameter (2 cm^2) were placed in Petri dishes and inoculated with 50 μL of microorganisms at a concentration of 1.0×10^7 CFU/mL and incubated for 30 min at room temperature (≈21 °C). Then, the samples were transferred to falcons with 5 mL of PBS (NaCl 8 g/L (Sigma Aldrich, St. Louis, USA), KCl 0.2 g/L (Panreac, Barcelona, Spain), Na_2HPO_4 1.44 g/L (Panreac, Barcelona, Spain), KH_2PO_4 0.24 g/L (Panreac, Barcelona, Spain), pH 7.4), and thoroughly vortexed for more than 1 min to homogenize. This suspension was collected, serial diluted and plated in tryptic soy agar Petri dishes containing 30 g/L of tryptic soy broth (Liofilchem, Italy) and 15 g/L of agar (VWR, Chemicals BDH, Portugal). Then, the CFU/mL was determined after an incubation of 16 h at 37 °C, and the log reduction was determined for equation (3) (Eq. (3)). The assay was performed in triplicate.

$$\log_{-}(\text{reduction}) = \log_{-}(\varnothing) - \log_{-}(s) \quad \text{Eq. (3)}$$

were, $\log_{\varnothing}$ is average of CFU/mL control log, and $\log_s$ is average of sample CFU/mL log.

2.11. In vitro cellular viability

The 3T3-L1 fibroblasts (ATCC, USA) were cultured in Dulbecco's modified eagle medium (DMEM) medium supplemented with 10 % (v/v) fetal bovine serum (HyClone, USA) and 1 % (v/v) penicillin and streptomycin (HyClone, USA). The cells were kept at 37 °C in a 95 % humidified atmosphere and 5 % CO_2. Flasks were passaged (passaged 19) when fibroblasts were 80–90 % confluent. Exposure (3 min) to trypsin-ethylenediaminetetraacetic acid (EDTA) 0.25 % (w/v) (Corning, USA) was used to release cells adhered to the surface of the flask. All experiments were performed in triplicate for each treatment and control group. Metabolic activity was determined by reducing the thiazolyl blue tetrazolium bromide (MTT) compound assay. Then, 10,000 cells were seeded in each well and incubated at 37 °C in a 95 % humidified atmosphere and 5 % CO_2. Cell viability was evaluated after 24, 48, and 72 h of incubation. In each measurement, the culture medium was discarded, and the cells were washed with 200 μL of Dulbecco's phosphate buffered saline (DPBS) (Gibco, USA) for 5 min to eliminate the remains of the medium and the detached cells, which was then removed. Subsequently, 150 μL of MTT solution in DMEM without phenol red (Gibco, USA) was added to each well and incubated for 1–2 h. Once the time has elapsed, the MTT must be removed. Finally, 150 μL of isopropanol is added to each well, the 96-well plate is inserted into the microplate reader model 680 UV (BioRad Laboratories, Inc., USA), it is shaken for 10 s, and the absorbance (OD) reading is taken at 570 nm. Well plates without extracts containing the same initial cell concentration were used as a control.

To observe cell morphology and to count cells attached to chamber cell culture Slide 8 wells, the cell cytoplasm and nuclear DNA were stained with Rhodamine Phalloidin (ThermoFisher, USA) and Hoechst-33342 (Merk, Germany), respectively. The cells were fixed with a 3.7 % (v/v) formaldehyde solution for 60 min and then rinsed in PBS to remove the formaldehyde. After that, attached cells were incubated in a Triton X-100 solution (0.1 % v/v) for 15 min and washed several times with PBS to remove the Triton X-100. The cell cores were stained with (blue) Hoechst-33342 at 4 °C overnight, and cell cytoskeletons were stained with (red-orange) Rhodamine Phalloidin (300 μM solution, for 30 min at room temperature). The stained cells were observed under a Leica SP2 confocal microscope (Leica, Germany).

2.12. Statistical analysis

The statistical software IBM SPSS Statistics 25, GraphPad Prism 9 and OriginPro 8.5 were used for data analysis. Data normality was analyzed using the Shapiro–Wilk test. All experiments were expressed as mean ± standard deviation. The comparison between the different groups was made using the ANOVA test. The Tukey post-hoc test was used to compare the mean of the data in different groups. A $p < 0.05$ was considered as a statistically significant level. Different superscript letters in tables and asterisks in figures indicate significant differences among groups.

3. Results and discussion

3.1. Extracts study and characterization

3.1.1. Extracts development

B. globosa leaves were collected in a semi-rural sector between the communes of Cunco and Freire (La Araucanía Region, Chile). The first collection was made on July 18, 2021, in winter (39°00′07.3″S 72°19′18.7″O 226 m above sea level (masl)). The bushes were approximately 1–1.5 m high without flowers or fruits. The second collection was made on November 28, 2021, in spring in the same sector. The bushes median approximately 1–1.8 m high, with the presence of orange flowers but no fruits. Sparse surrounding vegetation at both collection sites. The samples were identified by Dr. Alicia Marticorena Garri, curator of the Herbarium CONC of the Department of Botany of the Faculty of Natural and Oceanographic Sciences of the University of Concepción, Chile, and the vouchers are 193219 (first collection) and 193220 (second collection).

Four types of *B. globosa* extracts were developed: an aqueous extract collected in winter (M1), a hydroalcoholic extract (ethanol/water 50:50 v/v) collected in winter (M2), an aqueous extract of collected in spring (M3), and a hydroalcoholic extract (ethanol/water 50:50 v/v) collected in spring (M4). The extraction yields were determined to be approximately 20 % for all four types of extracts, showing no significant differences [42]. developed extracts of *B. globosa* by boiling the leaves in distilled water for 2 h, reporting an extraction yield of 2 % [40]. reported extraction yields of *B. globosa* leaves using apolar solvents: n-hexane (2.4 %), dichloromethane (1.6 %), and methanol (8.6–9.6 %). Generally, the literature indicates that the use of organic solvents such as methanol, ethanol, dichloromethane, or hexane predominates [15,18,43], which allows for the production of fractionated extracts facilitating compound

identification. However, in this work, extraction methods using water or ethanol/water (50:50 v/v) were chosen to obtain extracts with a broad range of compounds, with a higher yield.

3.1.2. Extracts development

The FTIR spectra of the *G. tinctoria* and *B. globosa* extracts are shown in Fig. 1. In the case of the *G. tinctoria* extract, the band at 3220 cm^{-1} suggests the presence of = CH- unsaturated (alkenes, aromatic). The 1600 cm^{-1} band corresponds to aromatic compounds with the presence of the conjugated double bond C=C [44,45] and the 1707 cm^{-1} band corresponds specifically to the COOH acid group [46]. The *B. globosa* extract showed a very broad band around 3464 cm^{-1} that may be due to the OH stretching vibrations of the phenols and carboxylic groups in the extract [47]. Even though the samples were stored in a desiccator after lyophilization, all of them show a marked wide band between 3000 and 3600 cm^{-1}, which could also correspond to the OH of the water. Chromone carbonyl absorption and aromatic C=C double bonds are observed at 1598 cm^{-1} [48], although it is also possible that they are N-H bending bands associated with amines [49,50]. N-H bending bands of amines are common and expected signals in infrared spectra of crude plant leaf extracts, reflecting the presence of nitrogenous compounds such as alkaloids and amino acids. No great differences are observed in the spectra of M1, M2, M3 and M4, which suggests that the season where the plant material was collected, nor if the extraction medium is aqueous or hydroethanolic, does not greatly influence the functional groups identified.

3.1.3. HPLC analysis

HPLC fingerprinting of *B. globosa* extracts M1, M2, M3, and M4 are shown in Fig. 2. The HPLC chromatograms show the peaks present in the samples, particularly peaks A, B, and C, which correspond to forsitoside B, verbascoside, and luteolin 7-o-glucoside, respectively. Extracts M1 and M2 exhibited the highest activity of these biomarkers, while M3 and M4 showed lower levels of these compounds compared to other compounds. This suggests that *B. globosa* leaves present a higher number of phenolic compounds in winter than in spring. This could be explained by the fact that plants are exposed to greater environmental stress in winter than in spring, such as low temperatures or heavy rainfall, which would induce plants to produce more phenolic metabolites as a protective mechanism. These results are consistent with those reported by Refs. [17,51], where the same compounds were identified. In fact, the authors established that verbascoside, forsitoside B, and luteolin 7-O-glucoside are three of the most important phenolic compounds present in the leaves of *B. globosa*. Authors such as [17,40,44] link the presence of verbascoside and luteolin 7-O-glucoside as possible factors responsible for the anti-inflammatory, analgesic, and antioxidant activities reported in *B. globosa* extracts.

The profile of compounds detected in *B. globosa* extracts is the same as that published by Ref. [17] in that study, the authors detected 25 compounds, of which they could only identify 17. In our study, we propose the identification of 4 of the compounds that had not been previously identified (peak 22 to 25), which is detailed in Table 1. These compounds belong to the phenylpropanoid glycoside family, recognized for their antioxidant, anti-inflammatory, and antimicrobial properties [18,43].

Peak 22: Betonioside E. This compound is a phenolic glycoside related to other medicinal species such as *Betonica officinalis* and has recently been identified in *B. globosa* using advanced purification methods [18]. Betonioside E possesses remarkable antioxidant properties, attributable to its structure rich in phenolic hydroxyl groups, which allows it to effectively neutralize free radicals. Its presence in this species contributes to the traditional therapeutic value attributed to the plant [43].

Peak 23: β-OH-Forsytoside B methyl ether, this is a methylated form of forsytoside B, with an additional hydroxyl group. Modifications such as methylation can improve the compound's chemical stability and modify its bioavailability. Forsytoside derivatives have been described as effective anti-inflammatory and antimicrobial agents [18,52], and its presence in the *B. globosa* extract suggests a possible synergy with other phenolic compounds present.

Peak 24: Samioside, this structural isomer of forsytoside B shares a similar phenylpropanoid base, but its conformation may confer significant differences in its biological activity. Cytoprotective and antioxidant effects have been suggested, although more specific studies are required to determine its mechanism of action [18].

Peak 25: Stachyside A, a well-known isomer of forsitoside, reported

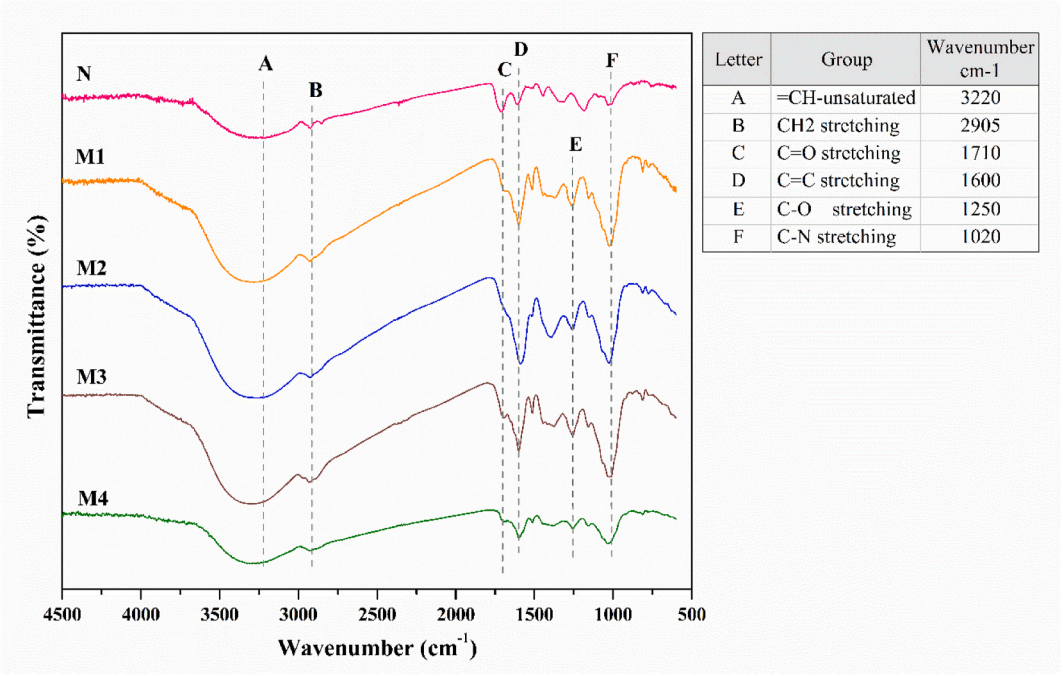

Letter	Group	Wavenumber cm-1
A	=CH-unsaturated	3220
B	CH2 stretching	2905
C	C=O stretching	1710
D	C=C stretching	1600
E	C-O stretching	1250
F	C-N stretching	1020

Fig. 1. FTIR spectra of *G. tinctoria* extract (N) and *B. globosa* extracts (M1, M2, M3 and M4).

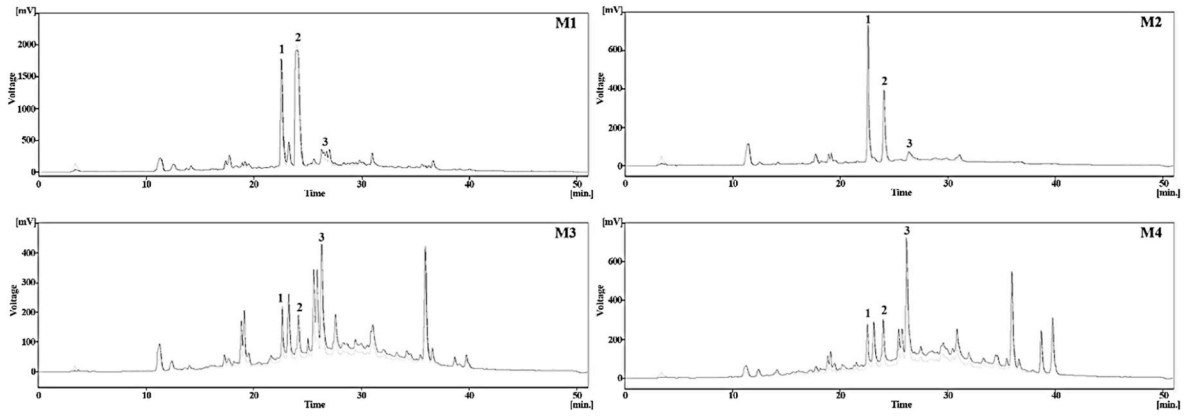

Fig. 2. HPLC-UV chromatogram of *B. globosa* extracts (M1, M2, M3 and M4). Peak numbers correspond to (1) Forsitoside B; (2) Verbascoside; and (3) Luteolin 7-O-glucoside.

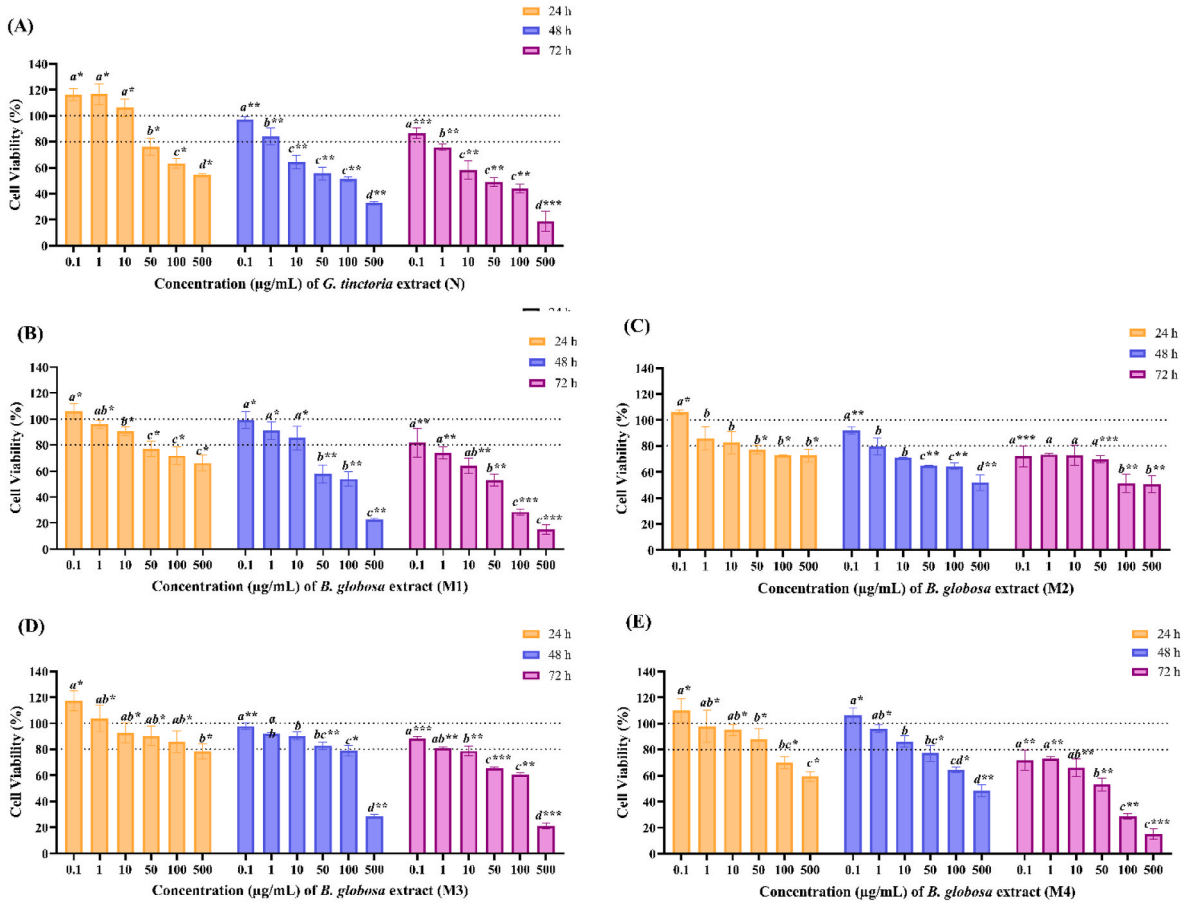

Fig. 3. Cell viability of 3T3-L1 fibroblasts (10,000 cells) and quantification of metabolic activity of live cells by MTT assay after exposure to extracts of *G. tinctora* N (A) and *B. globosa* M1 (B), M2 (C), M3 (D), and M4 (E) at different concentrations (500, 100, 50, 10, 1, and 0.1 µg/mL) for 24 h (dark gray), 48 h (light gray), and 72 h (white). Letters (a, b, c, d, and e) indicate significant differences between concentrations at the same time; asterisks (*) indicate significant differences between different times for the same concentration.

in other species such as *Stachys sieboldii*, this compound has demonstrated antioxidant activity and the ability to protect against oxidative damage induced by free radicals. Its presence complements the bioactive spectrum of the extract, in line with studies highlighting the anti-inflammatory and tissue effects of *B. globosa* extracts [43,52].

3.1.4. Total polyphenols content

A gallic acid calibration curve determined the total polyphenol content (Table 2). The values obtained for the four *B. globosa* extracts (M1, M2, M3 and M4) were similar to each other, while the *G. tinctoria* (N) extract showed a significantly higher content ($p = 0.0001$) [53]. reported a total polyphenol content of 520 ± 30 mg GAE/g of dry extract in the leaves of *G. tinctoria*. A lower content is observed when comparing this value to the 251.74 ± 15.88 mg GAE/g obtained in petiole dry extract. However, compared to the results from Ref. [54], who reported 106.84 ± 1.28 mg GAE/g of dry leaf extract, the values in this study are

Table 1
Identification of targeted phenolic compounds from *B. globosa* extracts (M1 – M4) by HPLC.

Peak	RT min	Formula	Experimental (observed) mass	Mass (monoisotopic mass) calculated	Error ppm	[M − H]- m/z	MS-MS fragments	Proposed compound
22	54.08	$C_{35}H_{46}O_{20}$	786.3	786.3	1.38	785.3	623.2, 547.2, 463.2, 378.9, 291.1, 207.1	Betonioside E
23	54.38	$C_{35}H_{46}O_{20}$	786.3	786.3	1.35	785.3	547.2, 463.2, 341.1, 207.1, 163.0	B-OH-Forsitoside B methyl-ether
24	57.03	$C_{34}H_{44}O_{19}$	756.3	756.2	3.46	755.2	709.2, 465.0, 405.0, 341.0, 285.0	Samioside
25	57.67	$C_{34}H_{44}O_{19}$	756.3	756.2	3.42	755.2	709.2, 593.1, 541.0, 497.0	Stachyoside A

Table 2
Total polyphenol content (mg GAE/g dry extract) by Folin-Ciocalteu method and antioxidant activity (mg TroloxE/mg dry extract; % inhibition and IC_{50}) of *G. tinctoria* (N) and *B. globosa* (M1, M2, M3 and M4) extracts by DPPH method.

Extracts	mg GAE/g dry extract			mg TroloxE/mg dry extract			% Inhibition	IC_{50} (μg/mL)
N	251.74[a]	±	15.88	2019.33[a]	±	23.57	76.4	305
M1	106.70[b]	±	21.49	352.13[b]	±	11.34	54.2	430
M2	77.31[b]	±	21.39	117.89[d]	±	5.24	17.8	1309
M3	105.27[b]	±	27.46	219.28[c]	±	4.28	34.8	669
M4	103.02[b]	±	25.40	90.94[d]	±	5.56	13.9	1677

a, **b, c** and **d** express statistically significant differences, with the formation of subsets.

Table 3
MICs and MBC_{50}/MFC_{50} of natural extracts N, M1, M2, M3, and M4 against *S. aureus*, *P. aeruginosa,* and *C. albicans*.

Extracts	MICs (mg/mL)			MFC_{50}/MBC_{50} (mg/mL)		
	S. aureus	***P. aeruginosa***	***C. albicans***	***S. aureus***	***P. aeruginosa***	***C. albicans***
N	0.125	0.500	>1.00	0.500	>2.00	>2.00
M1	0.250	>1.00	>1.00	>1.00	>2.00	>1.00
M2	0.500	>1.00	>1.00	>1.00	>2.00	>2.00
M3	0.500	>1.00	>1.00	>1.00	>2.00	>2.00
M4	0.250	>1.00	>1.00	>1.00	>2.00	>2.00

higher. Regarding *B. globosa* extracts [55], reported a content of 63.37 ± 2.24 mg GAE/g of dry flower extract, indicating that the values obtained in under study for leaves are higher. Nevertheless [15], developed *B. globosa* leaf extracts using the Soxhlet method with high-temperature distillation and reported a total polyphenol content of 19.3 mM (GAE), which is approximately equivalent to 1622.19 mg GAE/g of dry matter, a value much higher than determined in this study. The comparison with previous work shows variability in the results, which could be attributed to factors such as the extraction method, plant origin, or environmental conditions during growth.

3.1.5. *In vitro antioxidant activity*

The antioxidant activity (Table 2) was calculated using the Trolox calibration curve with $R^2 = 0.9988$. The antioxidant activity measured in the five extracts analyzed showed results with statistically significant differences. The highest value being that of the *G. tinctoria* extract (N) (2019.33 ± 23.57 mg TroloxEq/mg dry extract), followed by the *B. globosa* extracts (M1) (352.13 ± 11.34), M3 (219.28 ± 4.28) and finally M2 (117.89 ± 5.24) and M4 (90.94 ± 5.56) [56]. carried out the determination of the antioxidant activity by the reduction of the DPPH radical of different structures of *G. tinctoria*. Their results showed 220.9 ± 13.3 (Roots); 542.3 ± 86.1 (Inflorescences); 705.0 ± 26.1 (young leaves); 515.2 ± 65.9 (adult leaves) mg TroloxE/g dry extract. It is observed that the results obtained by Ref. [56] are well below that obtained in this investigation for the N extract, however these differences could be generated by methodological variations, since in that publication the details of the methodology used to determine the antioxidant activity by the reduction of the DPPH radical are not shown [11]. mentioned that the DPPH radical has a high reaction selectivity since it does not react with flavonoids that lack OH groups in a B-ring or with aromatic acids that contain a single OH group. Therefore, the high antioxidant capacity measured by the DPPH technique suggests a high efficiency on the part of the polyphenols present in the plant matrices analyzed. On the other hand, a certain correlation was observed between the number of total polyphenols measured in the extracts, with the subsequent antioxidant activity determined, being the extract N, the one with the significantly higher antioxidant activity and the extract with the highest total polyphenol content. On the contrary, the M2 extract presented the lowest antioxidant activity and the lowest number of total polyphenols. In this sense [17], mentioned a direct correlation between antioxidant activity and polyphenol content determined by the Folin-Ciocalteau method, reinforcing this knowledge.

3.1.6. *In vitro antimicrobial activity*

The antimicrobial activity of the natural extracts studied (N, M1, M2, M3, and M4) was also evaluated by the MIC and MBC_{50}/MFC_{50} method. The MIC results (Table 3) demonstrated a considerable reduction in OD at concentrations ranging from 0.125 to 0.500 mg/mL for all extracts evaluated against *S. aureus*. However, no considerable activity was observed against *P. aeruginosa* and *C. albicans*, except for extract N, which exhibited a noticeable reduction in OD against *P. aeruginosa* at a concentration of 0.5 mg/mL. Notably, no decrease in OD was detected for C. albicans in any of the tested conditions.

The MBC/MFC_{50} values for the microorganisms under investigation exceeded 1 or 2 mg/mL (with a log reduction of less than 2 against *S. aureus* and zero against *P. aeruginosa* and *C. albicans*). In contrast, a concentration of 0.5 mg/mL was effective against *S. aureus*, resulting in a log reduction of 4.4 (Table 4). Natural extracts did not exhibit antimicrobial activity against *S. aureus*, *P. aeruginosa*, and *C. albicans* at concentrations lower than 1 or 2 mg/mL. Previous analysis of the extracts identified compounds with antioxidant and antimicrobial activity reported as hydrolyzed tannins (dicaloylglucose derivatives), flavonoids

Table 4
Antimicrobial activity in $Log_{reduction}$ of *G. tinctoria* and *B. globosa* extracts evaluated at different concentrations (0.016–2.0 mg/mL) against *S. aureus*, *P. aeruginosa*, and *C. albicans*.

Extracts	S. aureus		P. aeruginosa		C. albicans	
	[Extract] (mg/mL)	$Log_{reduction}$ (CFU/mL)	[Extract] (mg/mL)	$Log_{reduction}$ (CFU/mL)	[Extract] (mg/mL)	$Log_{reduction}$ (CFU/mL)
N	0.5	4.4	2.0	0	2.0	0
M1	1.0	1.5	2.0	0	1.0	0.1
M2	1.0	1.2	2.0	0	2.0	0
M3	1.0	1.5	2.0	0	2.0	0.7
M4	1.0	1.8	2.0	0	2.0	0.9

Table 5
Table with magnitudes assigned to all the independent variables for the development of electrospun fibers with *G. tinctoria* and *B. globose* extracts.

Fibers Samples	*G. tinctoria extract* (mg/mL)	*B. globose* extract (mg/mL)	PCL (% w/v)	Voltage+ (kV)	Flow rate (mL/h)	Distance to collector (cm)	Collector rotation (rpm)
P1	0.1	0.1	14	25	2	20	50
P2	1.0	0.1	14	25	2	20	50
P3	0.1	1.0	14	25	2	20	50
P4	1.0	1.0	14	25	2	20	50
P5	0.5	0.5	14	25	2	20	50
P6	1.0	0	14	25	2	20	50
P7	0	1.0	14	25	2	20	50
P8	0	0	14	25	2	20	50

(quercetin) and phenolic acids (gallic acid and caffeic acid) in the extract of *G. tinctoria* (N); and Forsythoside B, Verbascoside and Luteolin 7-O-glucoside, in the extracts of *B. globosa* (M1 – M4) [57–60]. Nonetheless, the results obtained against *P. aeruginosa* and *C. albicans* do not seem to coincide with the literature. This may be attributed to the concentrations under study, extraction methods, and variations in plant sources.

3.1.7. *In vitro metabolic activity and cellular viability*

The cell viability of 3T3-L1 fibroblasts (ATCC, USA) (10,000 cells) was assessed by MTT assay, which quantifies the metabolic activity of living cells. Cells that reduce MTT by the action of enzymes such as succinate dehydrogenase and produce the insoluble purple/blue formazan crystal. The fibroblasts were exposed to different concentrations (0.1, 1, 10, 50, 100 and 500 μg/mL). The negative control (without extract) was considered 100 % cell viability, and the results were compared according to this criterion. 80 % was considered the minimum acceptable cell viability (dotted line) [61], in the same way that when cell viability was above 100 %, a dose that enhances cell reproduction was considered.

As shown in Fig. 3, cell viability changes depending on the cell line, the extract type, and the applied concentration. The most notable trend was observed with extract N (Fig. 3a), where viability increased at low concentrations (0.1, 1, and 10 μg/mL) but decreased sharply from 50 μg/mL onward. In addition to this dose-dependent effect, a clear time-dependent trend was detected across 24, 48, and 72 h, with significant inter-time differences indicated by asterisks. These findings confirm that fibroblast responses evolve not only with concentration and extract type but also over time, reflecting the combined influence of phenolic compounds and exposure dynamics [62]. reported that the fibroblasts viability is directly proportional to the concentration of natural extracts (*Tropaeolum majus* and *Salvia officinalis*). The effect of extracts M1, M2, M3 and M4 (Fig. 3 (b, c, d and e)) showed a trend similar to extract N, i.e, as the concentration of the extract increases, cell viability slight decreases. The concentration of 0.1 μg/mL produced a fibroblast viability above 100 % (M1, M2, M3 and M4). Despite the fact that at 24 h no significant differences in cell viability were observed at the different concentrations, at 48 and 72 h, the most important decrease was observed at the highest dose (500 μg/mL).

Fig. 4a and b and c showed confocal images of 3T3-L1 fibroblasts whereas cultured in an 8-well cell culture chamber. As observed in Fig. 5, the cells adhered to the surfaces preferred to grow along the plane and the cell morphology did not change significantly between the negative control (a) and the wells with extracts of *G. tinctoria* (b) or *B. globose* (c).

In a study published by Ref. [39] the researchers reported increased fibroblast growth at low concentrations of *B. globosa* extract (0.05–1.0 μg/ml), but cytotoxicity at concentrations higher than 50 μg/ml. This is corroborated by Ref. [13] who also observed a slight effect on fibroblast proliferation at lower concentrations, although it was not significant,

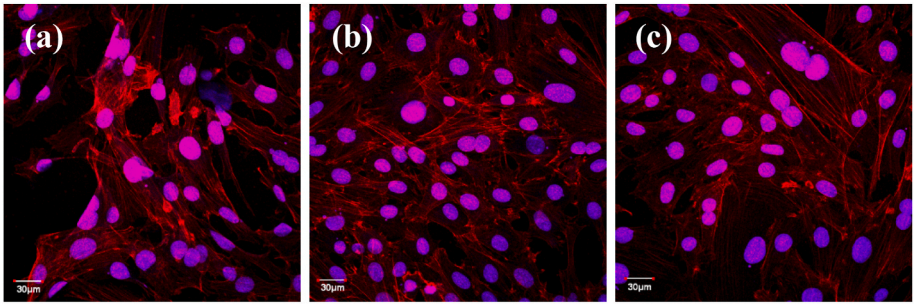

Fig. 4. Confocal images (40 ×) of 3T3-L1 fibroblasts (a, b and c) cultured on the chamber cell culture Slide 8 wells. (a) Fibroblasts without extracts, (b) Fibroblasts with *G. tinctoria* extract (N), (c) Fibroblasts with *B. globosa* extract (M1). Nuclei in blue/pink and cytoplasm in red. (For interpretation of the references to colour in this figure legend, the reader is referred to the Web version of this article.)

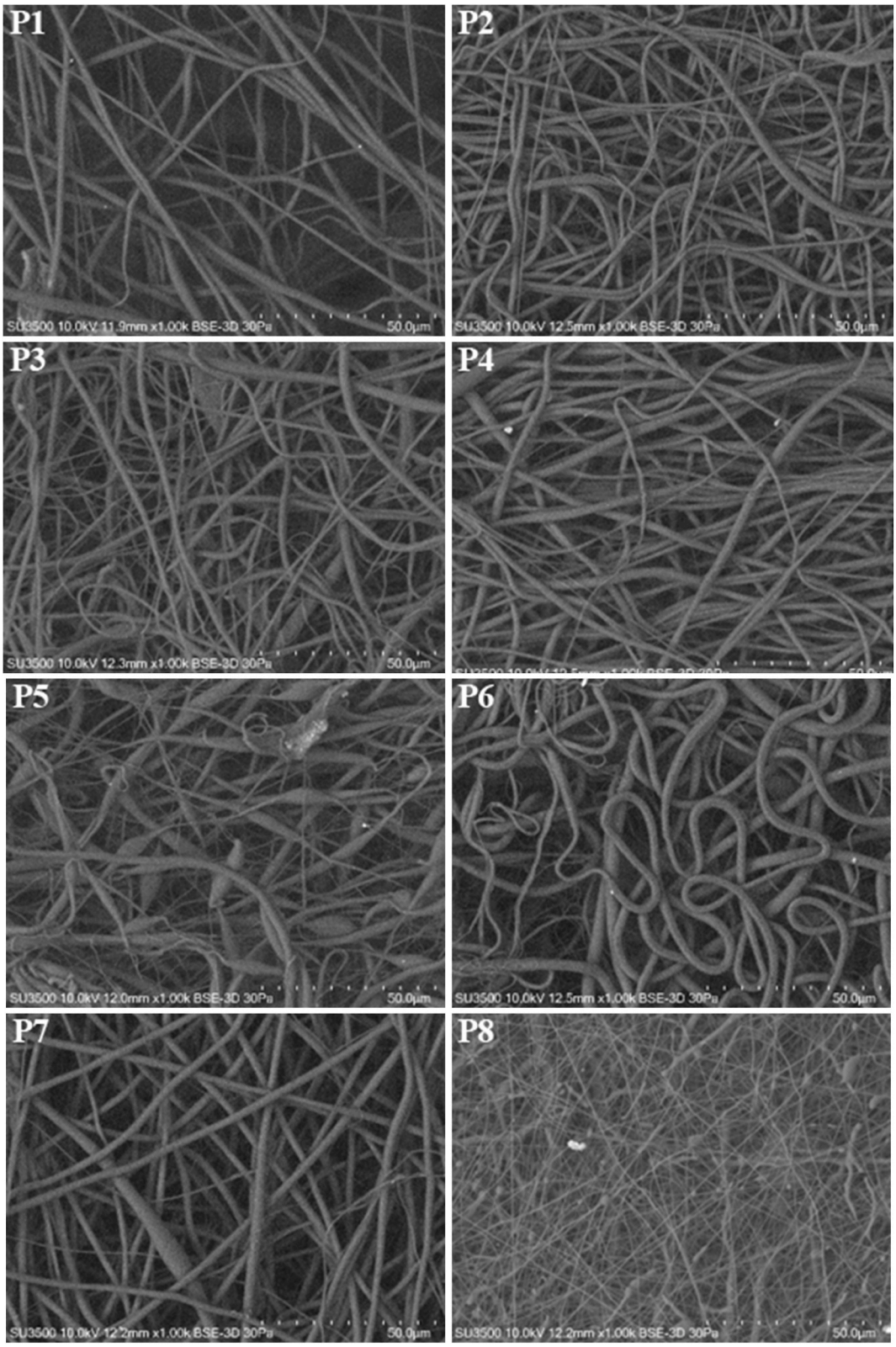

Fig. 5. SEM of the electrospun fibers from P1 to P8. Each image was conducted at 10 kV and a magnification of 1.00 k.

and higher concentrations appeared cytotoxic. Recently [63] demonstrated that concentrations higher than 2500 μg/mL of the methanolic extract of *Buddleja cordata* decreased cell viability of 3T3 fibroblasts by $\leq$ 83 % after 24 h of exposure. Studies on *B. globosa* indicate that its extracts have the potential to stimulate fibroblast growth and possess significant antioxidant properties. However, cytotoxicity at higher concentrations is a major limitation. These findings suggest that although *B. globosa* extracts may be beneficial for wound healing, it is crucial to determine optimal concentrations to avoid adverse effects. Thus, in this study, concentrations of 0.1, 0.5, and 1 mg/mL of *B. globosa*

M1 were selected to produce electrospun fibers.

3.2. Electrospun fibers SEM analysis

To produce micron-sized fibers, the impact of extract concentrations was examined, while the concentration of the polymer PCL dissolved in chloroform, the voltage and the distance between the needle and the collector were established thanks to preliminary tests where a constant electrospinning flow rate was sought. The conditions of the electrospinning process and the concentrations of PCL and the extracts are detailed in Table 5. It is important to note that for the development of these fibers, the extract of *B. globosa* M1 was used since this extract showed a higher quantity of total polyphenols, in addition to the highest antioxidant activity, compared to the rest of *matico* extracts (M2, M3 and M4).

The morphology index and diameter measurements of the fibers are shown in Table 6. Statistically significant differences were observed between the average diameters of the samples, with P8 being significantly different from all other groups. In addition, it can be observed that samples with higher morphology index (such as P2 and P3) tend to have a lower diameter, while samples with low index values (such as P5) have more variable diameters. However, it is impossible to state a solid trend due to the variability of the data and the weak correlation. The correlation coefficient between fiber diameter and morphology index is −0.28, indicating a weak negative correlation. This suggests that there is no clear relationship between these two variables in the available data. Nevertheless, SEM analysis revealed that the incorporation of plant extracts (P1–P7) significantly increased fiber diameter compared to the pure PCL control (P8), with up to a 2.6-fold rise. This effect is likely related to changes in solution viscosity and conductivity induced by phenolic metabolites, consistent with previous reports on blend electrospinning where hydrophilic compounds modulate fiber morphology.

with the formation of four subsets.

The voltage applied during electrospinning significantly affects fiber diameter, surface roughness, and pore volume. An application of a higher voltage (from 10 to 25 kV) increased fiber diameter and surface roughness, while specific surface area and wettability decreased [64]. Fig. 5 shows SEM images of samples P1 to P8, the fiber morphology is smooth, opaque and mostly regular. The electrospinning conditions produced fibers with very few imperfections, beads or artifacts, which is corroborated by the high morphological indices. Relative humidity and ambient temperature during electrospinning process also influence fiber morphology [65]. To avoid adding another variable that would affect fiber characteristics, the experiments were conducted under a relative humidity of 50 % and at a temperature of 25 °C.

3.3. Electrospun fibers mechanical properties

Three mechanical properties: elongation at break (%), tensile strength (MPa), and Young's modulus (MPa) were evaluated in the eight electrospun fiber samples (P1–P8) under constant process conditions (14 % w/v PCL, 25 kV, 2 mL/h, 20 cm, 50 rpm). The results are shown in Table 7. Samples without extract (P8) and with extracts at medium concentrations (P5) showed lower elongation compared to high concentrations of a single extract. P7 (*B. globosa* only) and P6 (*G. tinctoria* only) had the highest elongations (>624 %), suggesting that each extract alone increases ductility, possibly due to minimal interference between active compounds. The high combination (P4) of both extracts reduced elongation, which may indicate interactions between the bioactive compounds that affect the flexibility of the polymer matrix. P3 (high *B. globosa*, low *G. tinctoria*) had the highest strength (1.66 MPa). P5, P7, and P8 had lower strengths (~1.06–1.12 MPa), indicating that high concentrations of both extracts (P4) or neither (P8) do not necessarily imply greater strength. There may be a specific synergistic effect at particular ratios (such as P3) that improves mechanical strength. Higher stiffness was found in P4 (1.35 MPa) and P6 (1.26 MPa)—higher concentrations of *G. tinctoria* extract appear to correlate with greater stiffness. Samples without extracts or with only *B. globosa* (P7, P3) had the lowest moduli (~0.93–0.95 MPa), suggesting that *G. tinctoria* contributes more to structural stiffness.

The increased stiffness and strength observed in P3 and P4 is consistent with previous results showing that the addition of plant extracts improves these properties. For example, *Achillea millefolium* on PCL nanofibers increased modulus and strength by 5.7x and 5.5x, respectively [64,66,67]. Furthermore, studies with Inula graveolens showed similar increases in strength (from 1.6 to ~5.2 MPa) [68]. However, the elongation at break in our cases is much higher (>400 %) compared to other studies using nanosized PCL (~137 %), likely due to extract-polymer interactions that modulate structural flexibility. *G. tinctoria* (P2, P6): associated with a significant increase in modulus (1.26 MPa in P6), indicating that it provides stiffness through reinforcing polymeric interactions. *B. globosa* (P3, P7): promotes strong elongation (maximum in P7) and good strength (P3), but decreases stiffness, likely due to matrix plasticization. The combination of both extracts at high concentrations (P4) maximizes stiffness but compromises elongation, suggesting nonlinear interactions that support synergies or antagonisms between bioactive compounds. The inclusion of plant extracts likely alters the fibrillar microstructure and increases polymeric interaction, modulating the amorphous/crystalline matrix of PCL—an effect documented when parameters such as solvents or additives are modified [69]. Furthermore, changes in fiber diameter and morphology, influenced by the extracts, can also modify mechanical properties. These results indicate that, by varying extracts, it is possible to design PCL fibers with tailored mechanical properties: from flexible and elastic membranes (*B. globosa* only), to semi-rigid scaffolds (*G. tinctoria* only) or highly rigid structures (both high extracts), very important characteristics in the development of biomedical applications.

Table 6
Diameter measurement and morphology index of electrospun fibers P1 – P8.

Fibers Samples	Fiber Diameter (μm)			Morphology Index
P1	2.207[a]	±	0.561	0.85
P2	1.815[a]	±	0.382	1.00
P3	1.947[a]	±	0.593	0.90
P4	1.932[a]	±	0.615	0.70
P5	2.271[a]	±	1.090	0.05
P6	2.543[a]	±	0.844	0.80
P7	2.359[a]	±	0.562	0.85
P8	0.692[b]	±	0.188	0.60

[a] and **b** express statistically significant differences.

3.4. Electrospun fibers Physicochemical characterization

In the FTIR spectra of the eight fibers (Fig. 6) the characteristic PCL peaks are observed in three different regions, the first zone corresponding to the polymer fingerprint, where strong C=C bending predominates at 732 and 960 cm^{-1}, C-O-C stretching around 1170 cm^{-1} associated with the ester bonds, finally the band at 1470 cm^{-1} is observed which is attributed to the CH_2 bending. In the second zone, the C=O stretching is observed at approximately 1720 cm^{-1} corresponding to the carbonyl group. Finally, in zone three, the asymmetric stretching of CH_2 at 2867 cm^{-1} and CH_2 at 2940 cm^{-1} corresponding to the methylene groups is observed [70,71]. On the contrary, it is not possible to observe the characteristic peaks of the extracts. The unsaturated = CH at 3220 cm^{-1} disappears completely, as does the C=C at 1600 cm^{-1} and the C-N narrowing at 1020 cm^{-1}. As for CH_2 at 2905 cm^{-1}, it is possible that it overlaps with the PCL peaks in the region of 2940-2860 cm^{-1}. This phenomenon may be due to a combination of two factors: first, the relatively small amount of extract present in the fibers compared to PCL, and second, the fact that most of these extracts would be encapsulated within the fibers. Consequently, due to their limited presence on the fiber surface, the characteristic peaks of the extracts could not be

Table 7
Mechanical characterization of electrospun fibers (P1 – P8) with different *G. tinctoria* and *B. globose* extracts concentrations.

Fibers	Elongation at			Tensile			Young's		
Samples	Break (%)			Strength (Mpa)			Modulus		
P1	479.21	±	88.73	1.51	±	0.22	1.20	±	0.10
P2	577.50	±	29.90	1.56	±	0.16	0.98	±	0.11
P3	607.71	±	69.92	1.66	±	0.07	0.95	±	0.05
P4	413.96	±	46.43	1.58	±	0.17	1.35	±	0.08
P5	446.13	±	34.65	1.06	±	0.33	1.04	±	0.20
P6	624.83	±	91.72	1.42	±	0.10	1.26	±	0.10
P7	631.33	±	64.90	1.06	±	0.11	0.93	±	0.15
P8	496.92	±	52.77	1.12	±	0.08	1.03	±	0.14

Table 8
TGA, DSC and weight loss of electrospun fibers samples P1 – P8.

Fibers Samples	ΔH_m	T_m	C_x	T_b	Weight loss (%)		
	(J/g)	(°C)	(%)	(°C)	T_m	T_b	Residual weight
P1	36.75	63.4	26.38	417.4	0.05	97.23	2.80
P2	43.94	62.9	31.55	421.5	0.18	97.88	2.29
P3	41.41	62.5	29.73	425.3	0.10	98.54	1.56
P4	41.01	62.0	29.44	419.6	0.12	98.52	1.59
P5	43.01	62.3	30.88	422.2	0.21	98.55	1.69
P6	37.18	62.7	26.69	423.8	0.26	98.66	1.61
P7	42.88	62.8	30.78	421.9	0.12	98.56	1.55
P8	41.32	63.2	29.66	422.0	0.21	99.41	0.79

ΔH_m: Melting enthalpy; T_m: Melting point; C_x: Crystallinity; T_b: Boiling point.

identified.

The results of thermal characterization by differential scanning calorimetry (DSC) and thermogravimetric analysis (TGA) are summarized in Table 8. The parameters analyzed included the enthalpy of fusion (ΔH_m), melting temperature (T_m), degree of crystallinity (C_x), thermal degradation temperature (T_b), and percentage weight loss at T_m and T_b. The enthalpy of fusion (ΔH_m) of the fibers ranged from 36.75 J/g (P1) to 43.94 J/g (P2). Sample P2 presented the highest value, indicating greater crystalline structural order. In line with this, the degree of crystallinity (C_x) ranged from 26.38 % (P1) to 31.55 % (P2), calculated based on the theoretical ΔH_m for 100 % crystalline PCL (≈139.5 J/g). The presence of plant extracts, especially in P1 and P6, appeared to reduce crystallinity, which could be due to interference in the packing of polymer chains. However, formulations such as P2 and P5, with higher concentrations of *G. tinctoria*, showed values comparable to or higher than the control (P8), suggesting a favorable interaction or extract-induced plasticity. The melting temperature (T_m) remained relatively constant between samples (~62.0–63.4 °C), as expected in systems based primarily on PCL, and no significant shift attributable to the extracts was observed. The thermal degradation temperature (T_b), determined by the maximum of the first derivative of weight loss, ranged between 417.4 °C (P1) and 425.3 °C (P3). Samples with extracts did not show a significant decrease in thermal stability, indicating that their incorporation did not compromise the thermal integrity of the matrix. In fact, formulations such as P3 and P6 achieved T_b values higher than the control, suggesting a possible improvement in stability due to the antioxidant effect of the extract. Weight loss at T_m was minimal (0.05 %–0.26 %), indicating no significant evaporation of volatile components or water. At the degradation temperature (T_b), mass loss was greater than 97 % in all samples, with residues less than 2.8 %, with P8 (control) leaving the least residue (0.79 %). This suggests that most of the extracts and polymer were completely degraded, although a higher residue in samples such as P1 and P2 could indicate traces of inorganic or heat-resistant compounds of plant origin. DSC and TGA analyses performed on the PCL fibers with plant extracts revealed distinct effects on the crystallinity and thermal stability of the system. The addition of *G. tinctoria* and *B. globosa* extracts was observed to moderately affect the enthalpy of fusion (ΔH_m) and degree of crystallinity (C_x), although it did not significantly alter the melting temperature (T_m).

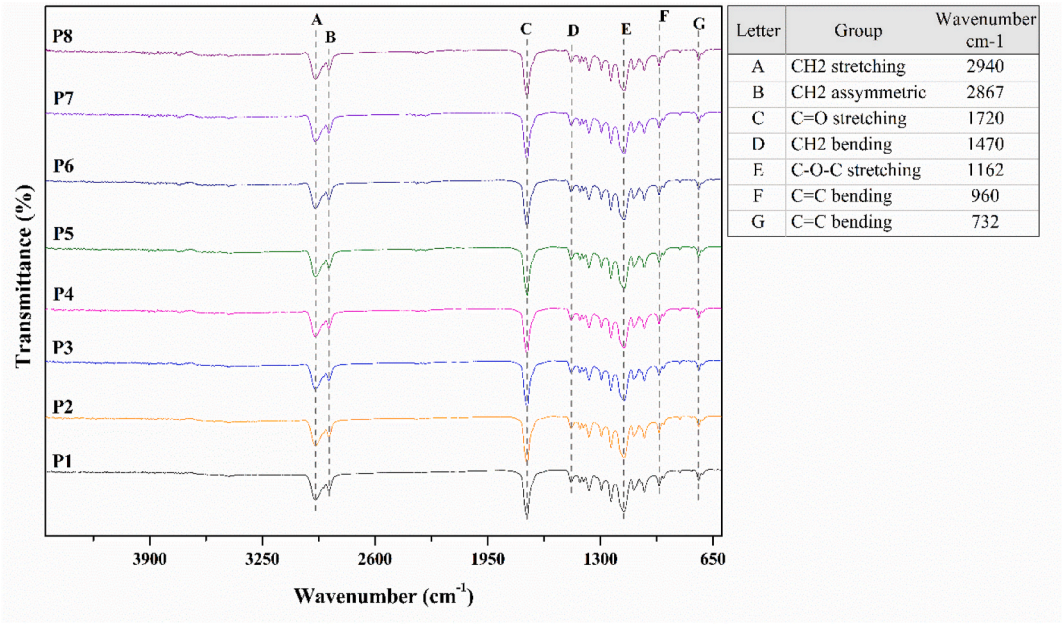

Fig. 6. FTIR spectra in transmittance (%) of electrospun fibers P1 to P8 from 4500 to 600 cm^{-1}.

These results are consistent with observations reported in the literature, since the reviewed studies indicate that PCL fibers exhibit high thermal stability [72,73]. The Tm range (~62–63.4 °C) is consistent with that reported for pure PCL, whose typical melting temperatures vary between 59 °C and 64 °C depending on molecular weight and processing [74]. The constancy of this value suggests that the main crystalline phase remains dominated by the polymer matrix, and that the extracts do not induce noticeable structural changes in the PCL crystal conformation. Regarding the degree of crystallinity, values between 26.38 % (P1) and 31.55 % (P2) indicate a semi-crystalline system, within the expected range for PCL (20–35 %) [74]. It has been documented that the addition of phenolic compounds or natural extracts can act as a plasticizing or steric interfering agent, reducing chain crystallization [66].

However, in this study, formulations such as P2 and P5 showed increases in crystallinity, suggesting that some bioactive compounds present could act as nucleants, promoting molecular ordering, as has been observed with certain polyphenols in similar systems [75]. Regarding thermal stability, the degradation temperature (T_b) remained between 417.4 °C and 425.3 °C, typical values for pure PCL degraded in an inert atmosphere [73]. The slight increase in T_b in samples such as P3 and P6 could be attributed to the antioxidant effect of the extracts, which can delay the thermal oxidation of the polymer, as has been described in PCL/natural antioxidant systems [72]. The low mass loss at T_m (<0.3 %) confirms that there was no significant evaporation or premature decomposition of the components. The solid residues at the end of the assay (0.79–2.8 %) are consistent with the presence of non-volatile or inorganic metabolites in the plant extract, such as condensed tannins or highly stable flavonoids [34].

3.5. Electrospun fibers in vitro antimicrobial activity

The antimicrobial activity of fibers produced with different concentrations of *G. tintoria* and *B. globosa* (0.1, 0.5, and 1 mg/mL) was evaluated against *S. aureus*, *P. aeruginosa, and C. albicans* (Fig. 7). All fibers exhibited a logarithmic reduction lower than 1 against evaluated bacteria, consequently classified as materials without antibacterial activity [40]. The anticipated antibacterial effect was not observed despite testing concentrations equal to or greater than the MBC_{50}. As the extracts were incorporated into the fibers, achieving antimicrobial activity would require concentrations exceeding the MBC_{50}. However, concentrations above the MBC_{50} (superior to 1 or 2 mg/mL) were not tested to mitigate the risk of potential cytotoxic effects. Conversely, the fiber containing a higher concentration of *G. tinctoria* and *B. globosa* extract (1 wt % each) (P4) demonstrated a significant antifungal effect against *C. albicans*, classifying it as a moderate disinfectant [40]. The absence of antifungal activity of P6 and P7, seems to corroborate the hypothesis that the combination of *G. tinctoria* and *B. globosa* extract displays a synergistic effect [76]. Furthermore, this synergistic effect is highly dependent on the concentration, as P5 also did not show any antifungal effect.

[77] showed that lipophilic extracts of the stem bark of *B. globosa* had antifungal activity at 125 μg/mL against three species of dermatophytic fungi (*Trichophyton rubrum*, *Trichophyton interdigitale*, and *Epidermophyton floccosum*), with buddledin A and buddledin B being the most active compounds. However, the extracts showed no activity at 1000 μg/mL against *A. niger*, *C. albicans*, *P. notatum*, *S. cerevisiae*, *S. brevicaulis*, and *S. dimidiatum*. No studies were found demonstrating that *B. globosa* extracts have antifungal activity against *C. albicans*; however, studies were found where bioproducts based on plants from the *Buddleja* genus did show some activity against *C. albicans* [78]. evaluated essential oils of *Buddleja polystachya* and showed antifungal activity against *C. albicans* at 0.5 mg/ml [79]. evaluated fractions and crude leaf extracts of *Buddleja salviifolia* (L.) and observed that the hexane and DCM fractions of the leaves showed the greatest activity against *C. albicans*, with MIC and MFC values of 390 μg/mL. No studies were found establishing the antimicrobial activity of *G. tinctoria* extracts against *C. albicans*. However [11], showed that the extract of this plant is rich in catechins (1344.97 mg/100 g dry weight) and epicatechins (1429.28 mg/100 g dry weight), which have been shown to inhibit the *in vitro* growth of *C. albicans* [80,81].

Electrospun PCL fibers have been extensively studied as antimicrobial dressing materials, especially when combined with bioactive agents. These fibers display a significant antimicrobial effect against relevant pathogenic bacteria, both Gram-positive and Gram-negative, when loaded with natural antimicrobial compounds, antibiotics, or peptides [82]. encapsulated nisin, a peptide with proven antimicrobial activity, in PCL fibers and demonstrated activity against *P. euroginosa* at 96 μg/mL and 2 μg/mL against *S. aureus* [83]. developed a multifunctional sandwich system based on sodium alginate and PCL where they encapsulated ampicillin. Antimicrobial assays showed effective antibiotic activity at 4 μg/mL against *S. aureus* and 64 μg/mL against *E. coli* [84]. developed PCL fibers on whose surface they immobilized the antimicrobial peptide pexiganan, which demonstrated an effect against *S. aureus* at 128 μg/mL, 16 μg/mL against *E. coli*, and 32 μg/mL against *A. baumannii* [85]. encapsulated microalgal peptides in PCL/κ-carrageenan fibers, and demonstrated antimicrobial effects against *E. coli* and *S. aureus* at 50 μg/mL [86]. encapsulated Cefazolin, a cephalosporin antibiotic, in PCL fibers and showed activity against *S. aureus* and *E. coli*. In another study [87], developed PCL/gelatin nanofibrous mats impregnated with *Gymnema sylvestre* encapsulated at 25 % (w/w) with respect to the polymers. In this study, they demonstrated that the presence of the extract effectively prevented bacterial colonization of gram-positive strains such as *S. aureus* and *S. epidermidis*. As can be seen, when using purified compounds, such as peptides or antibiotics, the antimicrobial effect occurs at concentrations mostly below 50 μg/mL. However, when crude or unpurified and fractionated extracts are used, the effective concentrations are usually higher, which could be a

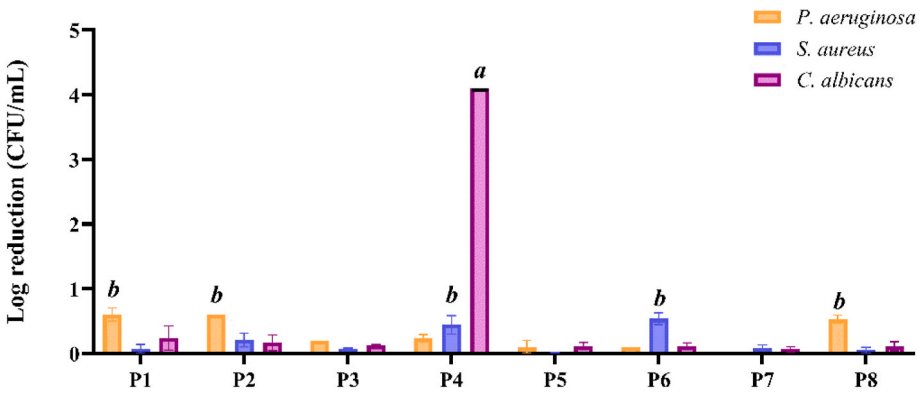

Fig. 7. Antimicrobial activity in $Log_{reduction}$ of electrospun fibers against *P. aeruginosa*, *S. aureus* and *C. albicans*.

drawback for technical, chemical, and biological reasons.

3.6. Electrospun fibers in vitro metabolic activity and cellular viability

The evaluation of 3T3-L1 fibroblast viability was carried out to assess the biocompatibility of fibers containing extracts of *G. tinctoria* and *B. globosa*, two native Chilean plants known for their antioxidant, anti-inflammatory, and wound-healing properties [43,88]. As shown in Fig. 3, cell viability varied depending on the cell line, the extract type, and the applied concentration. The most notable trend was observed with extract N (Fig. 3a), where viability increased at low concentrations (0.1, 1, and 10 μg/mL) but dropped sharply from 50 μg/mL onwards. In addition to this dose-dependent behavior, a clear time-dependent trend was observed across 24, 48, and 72 h, with significant inter-time differences indicated by asterisks, confirming that fibroblast responses evolve both with concentration and exposure duration. When extracts were incorporated into electrospun fibers (Fig. 8), similar time-dependent variations were observed. The formulations (P1–P8) differed in the concentration of each extract and were evaluated at 24, 48, and 72 h. Notably, formulation P1 (0.1 mg/mL of each extract) yielded the highest viability at 24 h (~130 %), significantly higher ($p < 0.0001$) than the control formulation without extract (P8), which reached only ~80 %. This positive effect was also evident in P2, P4, and P6, all containing G. tinctoria, suggesting that this extract plays a particularly important role in stimulating early fibroblast proliferation. These results support the notion that encapsulation enables a more sustained and modulated cellular response, consistent with the gradual release of phenolic compounds from the PCL matrix. The high initial viability may be attributed to phenolic compounds and tannins in *G. tinctoria*, which have been associated with tissue regeneration and cell. Formulation P4 (1 mg/mL of both extracts) also showed high viability (~130 %) and maintained favorable results over time. These findings indicate a possible synergistic effect between the two extracts, as P4 outperformed both P2 (high *G. tinctoria*, low *B. globosa*) and P3 (low *G. tinctoria*, high *B. globosa*), the latter of which presented viability below 100 % with no significant improvement over 72 h.

A general decreasing trend in viability over time was observed, likely due to compound degradation, nutrient depletion, or accumulation of metabolic byproducts [89]. Notably, P1 and P2 showed a significant drop after 48 h, potentially due to faster release of active compounds from the polymer matrix. Conversely, P4 and P5 maintained values above 80 % even at 72 h, suggesting a more sustained release profile and improved stability. Formulation P7, containing only *B. globosa*, showed lower viability (~85 % at 24 h) and did not improve with time. Despite the well-documented antimicrobial properties of this plant [43], this result may reflect concentration-dependent cytotoxic effects when used alone at higher doses. The results indicate that formulations containing *G. tinctoria* (P1, P2, P4, P6) were significantly more effective in enhancing fibroblast viability than those with only *B. globosa* (P3, P7). Among all, formulation P4 (1 mg/mL of both extracts) stood out for its high initial viability and sustained effect, making it the most promising candidate for wound healing or tissue engineering applications. These observations are consistent with previous studies highlighting the regenerative potential of *G. tinctoria* in skin models and the traditional use of *B. globosa* for wound healing [43]. However, the latter should be applied in optimized concentrations to avoid possible inhibitory effects on cell proliferation. The fibroblast viability results suggest that the phenolic extracts incorporated into the electrospun fibers promote early-phase cell proliferation. This effect is consistent with previous reports indicating that various polyphenols modulate signaling pathways such as ERK1/2 and PI3K/AKT, which are directly associated with cell survival, migration, and tissue regeneration [90–92].

Recently, dual-layer electrospun wound dressings loaded with IGF-1 and vanillin have been shown to enhance cell proliferation and accelerate wound healing *in vivo* [93]. Although our study focuses on cutaneous dressings containing phenolic extracts and on initial *in vitro* evaluations, scientific evidence indicates that bioactive nanofiber coatings can modulate cellular responses in a time-dependent manner and promote tissue regeneration, as demonstrated in 3D scaffolds coated with IGF-1-loaded nanofibers for calvarial defects. This parallel highlights the relevance of multifunctional designs and controlled release as complementary strategies to optimize cellular responses, and supports the need to incorporate future analyses of time-dependent viability, release modeling, and the exploration of signaling mechanisms underlying proliferation induced by phenolic compounds, without extrapolating osteogenic effects to cutaneous models [94].

In addition, while PCL enabled us to obtain stable and reproducible fibers, it is not a renewable or environmentally low-impact material. Recent studies have proposed the valorization of agricultural residues, such as cow manure-derived nanocellulose, for sustainable biomaterial production [95]. Integrating such renewable matrices with bioactive extracts could represent a significant step toward electrospun dressings that combine wound-healing functionality with improved environmental sustainability.

4. Conclusions

This study successfully developed and characterized electrospun fibers composed of PCL loaded with bioactive extracts of *G. tinctoria* and *B. globosa*, aimed at promoting applications in wound healing and skin tissue regeneration. The plant extracts were obtained using green extraction techniques (aqueous and hydroalcoholic), and their bioactive

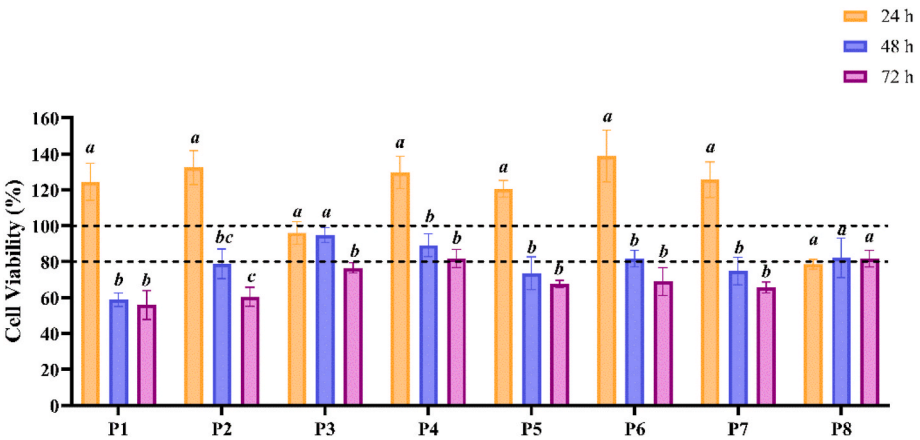

Fig. 8. Cell viability of 3T3-L1 fibroblasts (10,000 cells) and quantification of metabolic activity of live cells by MTT assay after exposure to the electrospun fibers (P1 – P8) for 24, 48 and 72 h. Different letters (a, b, c) indicate statistically significant differences between the different times for each sample.

profiles were confirmed by FTIR, HPLC, and antioxidant assays. Notably, the *G. tinctoria* extract showed the highest total polyphenol content and antioxidant activity, correlating with its more pronounced biological performance. The fibers demonstrated favorable morphological properties, thermal stability, and mechanical strength, with P4 (1 mg/mL of each extract) emerging as the most balanced formulation in terms of homogeneity, biocompatibility, and antifungal efficacy. FTIR analysis of the fibers confirmed the presence of characteristic PCL signals, while signals from the encapsulated extracts were not clearly visible, likely due to their internal incorporation. *In vitro* antimicrobial assays using *S. aureus* and *P. aeruginosa* exhibited a clear absence of antibacterial efficacy. However, a significant antifungal activity was observed for P4 against *C. albicans*, being classified as a moderate disinfectant. Interestingly, both individual extracts did not displayed any antifungal activity. In addition, when combined at the concentration of 0.5 mg/mL, also did not show any antifungal activity. However, when 1 mg/mL was used, the moderate disinfectant level was achieved. Indicating a possible synergistic effect of *G. tinctoria* and *B. globosa* extracts at a higher concentration. This is a highly interesting result, that requires further analysis to identify their active components. *In vitro* cell viability assays using 3T3-L1 fibroblasts confirmed the excellent biocompatibility of formulations containing *G. tinctoria*, with P4 maintaining high cell viability after 72 h of exposure. Overall, the results demonstrate that PCL fibers loaded with *G. tinctoria* and *B. globosa* extracts offer a promising platform for the development of bioactive wound dressing materials. Although this study focused primarily on evaluating the antioxidant, antimicrobial, and cytotoxic properties of electrospun fibers, it is important to recognize that the therapeutic success of a bioactive dressing also depends on the release kinetics of the incorporated compounds. The ability to control the release of phenolic metabolites over time is crucial for maintaining an effective concentration at the injury site and promoting sustained tissue regeneration. In this study, crude extracts were employed to assess the synergistic effect of their natural polyphenolic matrix in electrospun fibers. However, future research focused on fractionation and purified metabolites (e.g., verbascoside) could enhance bioactive potency, improve reproducibility, and support the clinical translation of these systems. Extract loading optimization and respective controlled release profiles should be performed in line with biocompatibility tests, and using widely validated approaches such as the Higuchi or Korsmeyer–Peppas models, which allow describing diffusion and relaxation mechanisms of the polymer matrix. Although electrospinning is a technique not embedded into the biomedical industry at full scale, this work represents an additional endorsement for its implementation in particular for active wound dressings, comprising native, undervalued, bioactive components.

CRediT authorship contribution statement

Jeyson Hermosilla: Writing – original draft, Validation, Methodology, Investigation, Funding acquisition, Formal analysis, Data curation, Conceptualization. **Cátia Alves:** Writing – review & editing, Methodology. **Andrea Zille:** Supervision, Methodology. **Jorge Padrão:** Writing – review & editing, Supervision, Methodology. **Claudia Sanhueza:** Methodology. **Edgar Pastene-Navarrete:** Writing – review & editing, Methodology. **Francisca Acevedo:** Writing – original draft, Visualization, Supervision, Resources, Investigation, Funding acquisition, Conceptualization.

Declaration of generative AI and AI-assisted technologies in the writing process

The authors used ChatGPT to assist in enhancing the language and clarity of certain sections of the manuscript. All content was subsequently reviewed and revised by the authors, who take full responsibility for the final version of the publication.

Declaration of competing interest

The authors declared that there are no personal conflict of interests influencing the work produced in this paper.

Acknowledgements

The authors would like to express their appreciation to *Programa de Doctorado en Ciencias de Recursos Naturales* (UFRO), Scientific and Technological Center for Bioresources (BIOREN-UFRO), *Centro de Excelencia en Medicina Traslacional* (CEMT-UFRO) and *Unidad de Tecnología y Procesos* (UTP-UFRO), Chile.

This work was supported by *Agencia Nacional de Investigación y Desarrollo de Chile (ANID)* scholarship N° 21190396, funded (partially) by *Universidad de La Frontera* (UFRO) Support PP24-0019, UFRO Thesis Completion Scholarship 2024, DIUFRO project PP24-0019, Nucleus Milenium Bioproducts, Genomic and Environmental Microbiology – BIOGEM (ANID-Milenio-NCN2023_054), and European Regional Development Fund through the Operational Competitiveness Program and the National Foundation for Science and Technology of Portugal (FCT) under the projects UID/CTM/00264/2020 of Centre for Textile Science and Technology (2C2T) on its components Base and Programmatic (https://doi.org/10.54499/UIDB/00264/2020 and https://doi.org/10.54499/UIDP/00264/2020).

Cátia Alves acknowledge FCT for the Ph.D. fellowship 2022.10454.BD and https://doi.org/10.54499/2022.10454.BD.

Abbreviations

PCL	polycaprolactone
SEM	scanning electron microscopy
ATR-FTIR	attenuated total reflection Fourier transform infrared
%T	percentage transmittance
HPLC	High-Performance Liquid Chromatography
HPLC–DAD-ESI/MS	high performance liquid chromatography equipped with photodiode array detection-mass
USA	United Stated of America
GAEq	equivalent milligrams of gallic acid
TGA	thermogravimetry
DSC	differential scanning calorimetry
DPPH	2,2-diphenyl-1-picrylhydrazyl free radical
MIC	minimum inhibitory concentration
MBC_{50}	half minimum bactericidal concentration
MFC_{50}	half minimum fungicidal concentration
CLSI	Clinical and Laboratory Standards Institute
EUCAST	European Committee on Antimicrobial Susceptibility Testing
AATCC	American Association of Textile Chemists and Colorists
CFU	colony forming unit
MHB	Mueller Hinton broth
OD	Optical density
PBS	phosphate buffer saline
DMEM	Dulbecco's modified eagle medium
EDTA	ethylenediaminetetraacetic acid
MTT	thiazolyl blue tetrazolium bromide
DPBS	Dulbecco's phosphate buffered saline
MASL	meter above sea level
ΔH_m	enthalpy of fusion
T_m	melting temperature
C_x	degree of crystallinity
T_b	thermal degradation temperature

Appendix A. Supplementary data

Supplementary data to this article can be found online at https://doi.org/10.1016/j.jddst.2025.107628.

Data availability

No data was used for the research described in the article.

References

[1] S. Chen, B. Liu, M.A. Carlson, A.F. Gombart, D.A. Reilly, J. Xie, Recent advances in electrospun nanofibers for wound healing, Nanomedicine 12 (11) (Jun. 2017) 1335–1352, https://doi.org/10.2217/nnm-2017-0017.

[2] T. Dai, Y.-Y. Huang, S.K. Sharma, J.T. Hashmi, D.B. Kurup, M.R. Hamblin, Topical antimicrobials for burn wound infections, Recent Pat. Anti-Infect. Drug Discov. 5 (2) (Jun. 2010) 124–151, https://doi.org/10.2174/157489110791233522.

[3] A.M. Lachiewicz, C.G. Hauck, D.J. Weber, B.A. Cairns, D. van Duin, Bacterial infections after burn injuries: impact of multidrug resistance, Clin. Infect. Dis. 65 (12) (Nov. 2017) 2130–2136, https://doi.org/10.1093/cid/cix682.

[4] M. Saaiq, S. Ahmad, M.S. Zaib, Burn wound infections and antibiotic susceptibility patterns at Pakistan Institute of Medical Sciences, Islamabad, Pakistan, World J. Plast. Surg. 4 (1) (2015) 9.

[5] S. Mickymaray, Efficacy and mechanism of traditional medicinal plants and bioactive compounds against clinically important pathogens, Antibiotics 8 (4) (2019) 257, https://doi.org/10.3390/antibiotics8040257.

[6] M.H. Al-Musawi, et al., Localized delivery of healing stimulator medicines for enhanced wound treatment, J. Drug Deliv. Sci. Technol. 101 (Nov. 2024) 106212, https://doi.org/10.1016/j.jddst.2024.106212.

[7] B. Casciaro, et al., Nigritanine as a new potential antimicrobial alkaloid for the treatment of staphylococcus aureus-Induced infections, Toxins 11 (9) (Sep. 2019) 511, https://doi.org/10.3390/toxins11090511.

[8] A. Toiu, L. Vlase, D.C. Vodnar, A.-M. Gheldiu, I. Oniga, Solidago graminifolia L. Salisb.(Asteraceae) as a valuable source of bioactive polyphenols: HPLC profile, in vitro antioxidant and antimicrobial potential, Molecules 24 (14) (2019) 2666, https://doi.org/10.3390/molecules24142666.

[9] S. Hebel-Gerber, et al., Chilean rhubarb, Gunnera tinctoria (Molina) mirb. (Gunneraceae): uhplc-esi-orbitrap-ms profiling of aqueous extract and its anti-helicobacter pylori activity, Front. Pharmacol. 11 (Jan) (2021), https://doi.org/10.3389/fphar.2020.583961.

[10] G. Petzold, G. Catril, C. Duarte, Caracterización fisicoquímica de pecíolos del pangue (Gunnera tinctoria), Rev. Chil. Nutr. 33 (3) (2006) 539–543, https://doi.org/10.4067/S0717-75182006000500010.

[11] P. Velásquez, K. Riquelme, F. Leyton, A. Giordano, M. Gómez, G. Montenegro, Antibacterial potential assessment of Nalca (Gunnera tinctoria Mol.) ethanolic extracts, Nat. Prod. Res. 35 (23) (2021) 5425–5428, https://doi.org/10.1080/14786419.2020.1777118.

[12] P. Zamorano, M. Morales, B.A. Rojano, Composición química proximal, capacidad antioxidante y actividad antifúngica de peciolo de nalca (Gunnera tinctoria), Inf. Tecnol. 29 (2) (2018) 185–194, https://doi.org/10.4067/S0718-07642018000200185.

[13] S. Bustamante Delgado, et al., Fundamentación preclínica del uso etnomédico de matico (Buddleja globosa Hope), Revista de fitoterapia 15 (2015) 37–51, 1576–0952.

[14] P.J. Houghton, P.J. Hylands, A.Y. Mensah, A. Hensel, A.M. Deters, In vitro tests and ethnopharmacological investigations: wound healing as an example, J. Ethnopharmacol. 100 (1–2) (Aug. 2005) 100–107, https://doi.org/10.1016/j.jep.2005.07.001.

[15] M. Fuentes, C. Sepúlveda, M. Alarcón, I. Palomo, E. Fuentes, Buddleja globosa (matico) prevents collagen-induced platelet activation by decreasing phospholipase C-gamma 2 and protein kinase C phosphorylation signaling, J. Tradit. Complement. Med. 8 (1) (Jan. 2018) 66–71, https://doi.org/10.1016/j.jtcme.2017.02.005.

[16] M. Suwalsky, J. Duguet, H. Speisky, An In vitro Study of the antioxidant and antihemolytic properties of Buddleja globosa (Matico), J. Membr. Biol. 250 (3) (Jun. 2017) 239–248, https://doi.org/10.1007/s00232-017-9955-0.

[17] M.E. Letelier, et al., Safety profile and wound healing properties of a Standardized Buddleja globosa hope (Matico) Extract in Sprague-Dawley Rats, Rev Farmacol Chile 5 (2) (2012) 13–19.

[18] J. Torres-Vega, S. Gómez-Alonso, J. Pérez-Navarro, J. Alarcón-Enos, E. Pastene-Navarrete, Polyphenolic compounds extracted and purified from Buddleja Globosa hope (Buddlejaceae) leaves using natural deep eutectic solvents and centrifugal partition chromatography, Molecules 26 (8) (2021) 2192, https://doi.org/10.3390/molecules26082192.

[19] M. de Melo Brites, et al., Bromelain immobilization in cellulose triacetate nanofiber membranes from sugarcane bagasse by electrospinning technique, Enzyme Microb Technol 132 (Jan. 2020) 109384, https://doi.org/10.1016/j.enzmictec.2019.109384.

[20] J. Xue, T. Wu, Y. Dai, Y. Xia, Electrospinning and electrospun nanofibers: methods, materials, and applications, Chem Rev 119 (8) (2019) 5298–5415, https://doi.org/10.1021/acs.chemrev.8b00593.

[21] G. Rivero, M. Meuter, A. Pepe, M.G. Guevara, A.R. Boccaccini, G.A. Abraham, Nanofibrous membranes as smart wound dressings that release antibiotics when an injury is infected, Colloids Surf. A Physicochem. Eng. Asp. 587 (2020) 124313, https://doi.org/10.1016/j.colsurfa.2019.124313.

[22] M.O. Aydogdu, A. Delbusso, M. Edirisinghe, A battery powered approach to pressurised spinning: introducing the sustainability concept and shaping the future of fibre production methodologies, Appl. Energy 397 (Nov. 2025) 126331, https://doi.org/10.1016/j.apenergy.2025.126331.

[23] S. Amer, N. Attia, S. Nouh, M. El-Kammar, A. Korittum, H. Abu-Ahmed, Fabrication of sliver nanoparticles/polyvinyl alcohol/gelatin ternary nanofiber mats for wound healing application, J. Biomater. Appl. 35 (2) (Aug. 2020) 287–298, https://doi.org/10.1177/0885328220927317.

[24] M.O. Ilomuanya, et al., Development and characterization of collagen-based electrospun scaffolds containing silver sulphadiazine and Aspalathus linearis extract for potential wound healing applications, SN Appl. Sci. 2 (5) (May 2020) 881, https://doi.org/10.1007/s42452-020-2701-8.

[25] G. Jin, M.P. Prabhakaran, D. Kai, S.K. Annamalai, K.D. Arunachalam, S. Ramakrishna, Tissue engineered plant extracts as nanofibrous wound dressing, Biomaterials 34 (3) (Jan. 2013) 724–734, https://doi.org/10.1016/j.biomaterials.2012.10.026.

[26] R. Ramalingam, et al., Core–shell structured antimicrobial nanofiber dressings containing herbal extract and antibiotics combination for the prevention of biofilms and promotion of cutaneous wound healing, ACS Appl. Mater. Interfaces 13 (21) (2021) 24356–24369, https://doi.org/10.1021/acsami.0c20642.

[27] A.H. Mahmoud, et al., Nanoscale β-TCP-Laden GelMA/PCL composite membrane for guided bone regeneration, ACS Appl. Mater. Interfaces 15 (27) (Jul. 2023) 32121–32135, https://doi.org/10.1021/acsami.3c03059.

[28] D. Porrelli, et al., Antibacterial electrospun polycaprolactone membranes coated with polysaccharides and silver nanoparticles for guided bone and tissue regeneration, ACS Appl. Mater. Interfaces 13 (15) (Apr. 2021) 17255–17267, https://doi.org/10.1021/acsami.1c01016.

[29] K. Ren, Y. Wang, T. Sun, W. Yue, H. Zhang, Electrospun PCL/gelatin composite nanofiber structures for effective guided bone regeneration membranes, Mater. Sci. Eng. C 78 (Sep. 2017) 324–332, https://doi.org/10.1016/j.msec.2017.04.084.

[30] S. Metwally, et al., Surface potential and roughness controlled cell adhesion and collagen formation in electrospun PCL fibers for bone regeneration, Mater. Des. 194 (Sep. 2020) 108915, https://doi.org/10.1016/j.matdes.2020.108915.

[31] C. Sanhueza, et al., Osteoinductive electrospun scaffold based on PCL-Col as a regenerative therapy for Peri-Implantitis, Pharmaceutics 15 (7) (Jul. 2023) 1939, https://doi.org/10.3390/pharmaceutics15071939.

[32] C. Sanhueza, et al., One-step electrospun scaffold of dual-sized gelatin/poly-3-hydroxybutyrate nano/microfibers for skin regeneration in diabetic wound, Mater. Sci. Eng. C 119 (2021) 111602, https://doi.org/10.1016/j.msec.2020.111602.

[33] Y. Velioglu, G. Mazza, L. Gao, B.D. Oomah, Antioxidant activity and total phenolics in selected fruits, vegetables, and grain products, J. Agric. Food Chem. 46 (10) (1998) 4113–4117, https://doi.org/10.1021/jf9801973.

[34] W. Brand-Williams, M.E. Cuvelier, C. Berset, Use of a free radical method to evaluate antioxidant activity, LWT - Food Sci. Technol. (Lebensmittel-Wissenschaft -Technol.) 28 (1) (1995) 25–30, https://doi.org/10.1016/S0023-6438(95)80008-5.

[35] European Committee for Antimicrobial Susceptibility Testing (EUCAST) of the European Society of Clinical Microbiology and Infectious Diseases (ESCMID), Determination of minimum inhibitory concentrations (MICs) of antibacterial agents by broth dilution, Clin. Microbiol. Infection 9 (8) (Aug. 2003) ix–xv, https://doi.org/10.1046/j.1469-0691.2003.00790.x.

[36] J.M. Domingues, et al., Inhibition of Escherichia Virus MS2, surrogate of SARS-CoV-2, via essential oils-loaded electrospun fibrous mats: increasing the multifunctionality of antivirus protection masks, Pharmaceutics 14 (2) (Jan. 2022) 303, https://doi.org/10.3390/pharmaceutics14020303.

[37] B. Mehravani, A.I. Ribeiro, U. Cvelbar, J. Padrão, A. Zille, In situ synthesis of copper nanoparticles on dielectric barrier discharge plasma-treated polyester fabrics at different reaction pHs, ACS Appl. Polym. Mater. 4 (5) (2022) 3908–3918, https://doi.org/10.1021/acsapm.2c00375.

[38] J. Padrão, et al., Development of an ultraviolet-C irradiation room in a public Portuguese Hospital for safe re-utilization of personal protective respirators, Int. J. Environ. Res. Publ. Health 19 (8) (2022) 4854, https://doi.org/10.3390/ijerph19084854.

[39] T.D. Tavares, et al., Activity of specialized biomolecules against gram-positive and gram-negative bacteria, Antibiotics 9 (6) (2020) 314, https://doi.org/10.3390/antibiotics9060314.

[40] B. Vieira, J. Padrão, C. Alves, C. Silva, H. Vilaça, A. Zille, Enhancing functionalization of health care textiles with gold nanoparticle-loaded hydroxyapatite composites, Nanomaterials 13 (11) (May 2023) 1752, https://doi.org/10.3390/nano13111752.

[41] J. Padrão, et al., Bacterial cellulose-lactoferrin as an antimicrobial edible packaging, Food Hydrocoll. 58 (2016) 126–140, https://doi.org/10.1016/j.foodhyd.2016.02.019.

[42] A.Y. Mensah, et al., Effects of Buddleja globosa leaf and its constituents relevant to wound healing, J. Ethnopharmacol. 77 (2–3) (2001) 219–226, https://doi.org/10.1016/S0378-8741(01)00297-5.

[43] N. Backhouse, et al., Antinociceptive activity of Buddleja globosa (matico) in several models of pain, J. Ethnopharmacol. 119 (1) (Sep. 2008) 160–165, https://doi.org/10.1016/J.JEP.2008.06.022.

[44] I.D. Sideridou, E.C. Vouvoudi, G.D. Papadopoulos, Epoxy polymer Hxtal NYL-1™ used in restoration and conservation: irradiation with short and long wavelengths and study of photo-oxidation by FT–IR spectroscopy, J. Cult. Herit. 18 (2016) 279–289, https://doi.org/10.1016/j.culher.2015.09.005.

[45] W. Ketren, et al., The mechanism study of degradative solvent extraction of biomass by liquid membrane-Fourier Transform Infrared spectroscopy, Int. J. Pure Math. Sci. 12 (1) (2018) 9–13.

[46] S. Werle, et al., Phytoremediation as an effective method to remove heavy metals from contaminated area–TG/FT-IR analysis results of the gasification of heavy metal contaminated energy crops, J. Energy Inst. 90 (3) (2017) 408–417, https://doi.org/10.1016/j.joei.2016.04.002.

[47] E. Carmona Ortíz, B. Escobar, V. Obando, Antimutagenic activity of Buddleja globosa extracts in the Drosophila wing-spot test, Fresenius Environ. Bull. 25 (12A) (2016) 5758–5764, vol. 25 (12A), no. 10184619, pp. 5758–5764.
[48] O. Deveoglu, E. Cakmakcı, T. Taskopru, E. Torgan, R. Karadag, Identification by RP-HPLC-DAD, FTIR, TGA and FESEM-EDAX of natural pigments prepared from Datisca cannabina L, Dyes Pigments 94 (3) (Sep. 2012) 437–442, https://doi.org/10.1016/j.dyepig.2012.02.002.
[49] R.S. Dangana, R.C. George, F.K. Agboola, The biosynthesis of zinc oxide nanoparticles using aqueous leaf extracts of *Cnidoscolus aconitifolius* and their biological activities, Green Chem. Lett. Rev. 16 (1) (Jan. 2023), https://doi.org/10.1080/17518253.2023.2169591.
[50] D. Susanna, R.M. Balakrishnan, J. Ponnan Ettiyappan, Comprehensive insight into the extract optimization, phytochemical profiling, and biological evaluation of the medicinal plant Nothapodytes foetida, Biocatal. Agric. Biotechnol. 42 (Jul. 2022) 102365, https://doi.org/10.1016/j.bcab.2022.102365.
[51] M. Friščić, F. Bucar, K. Hazler Pilepić, LC-PDA-ESI-MSn analysis of phenolic and iridoid compounds from Globularia spp, J. Mass Spectrom. 51 (12) (Dec. 2016) 1211–1236, https://doi.org/10.1002/jms.3844.
[52] J. Lu, X. Pu, Y. Li, Y. Zhao, G. Tu, Bioactive Phenylethanoid Glycosides from Buddleia lindleyana, Z. Naturforsch. B Chem. Sci. 60 (2) (Feb. 2005) 211–214, https://doi.org/10.1515/znb-2005-0214.
[53] C. Sabando, et al., Improvement of endothelial function by Gunnera tinctoria extract with antioxidant properties, Biol. Res. 53 (1) (Dec. 2020) 55, https://doi.org/10.1186/s40659-020-00322-2.
[54] P. Zamorano, B. Rojano, M. Morales, H. Magariños, P. Godoy, Biological and antioxidant activity of Gunnera tinctoria (Nalca), J. Med. Plants Res. 11 (17) (2017) 318–330, https://doi.org/10.5897/JMPR2017.6376.
[55] P. Zamorano-Aguilar, M. Morales, Y. Rivillas, J. López, B.A. Rojano, Antioxidant activity and cytotoxic effect of Chilean Buddleja globosa (Matico) and Ribes magellanicum (Zarzaparrilla) flower extracts, Acta Scientiarum Polonorum Hortorum Cultus 19 (6) (Dec. 2020) 59–70, https://doi.org/10.24326/asphc.2020.6.5.
[56] F. Fathi, et al., Exploring Gunnera tinctoria: from nutritional and anti-tumoral properties to phytosome development following structural arrangement based on molecular docking, Molecules 26 (19) (Sep. 2021) 5935, https://doi.org/10.3390/molecules26195935.
[57] P. Chavez Carvajal, et al., Chemical characterization and in vitro antibacterial activity of Myrcianthes hallii (O. Berg) McVaugh (Myrtaceae), a traditional plant growing in Ecuador, Materials 9 (6) (Jun. 2016) 454, https://doi.org/10.3390/ma9060454.
[58] J. Liu, et al., Protective effect of forsythoside B against lipopolysaccharide-induced acute lung injury by attenuating the TLR4/NF-κB pathway, Int. Immunopharmacol. 66 (2019) 336–346, https://doi.org/10.1016/j.intimp.2018.11.033.
[59] E. Sezen Karaoğlan, H. Hancı, M. Koca, C. Kazaz, Some bioactivities of isolated Apigenin-7-O-glucoside and Luteolin-7-O-glucoside, Appl. Sci. 13 (3) (2023) 1503, https://doi.org/10.3390/app13031503.
[60] C. Shi, et al., Verbascoside: an efficient and safe natural antibacterial adjuvant for preventing bacterial contamination of fresh meat, Molecules 27 (15) (2022) 4943, https://doi.org/10.3390/molecules27154943.
[61] P. Iso, 10993-5: 2009 (2009) Biological Evaluation of Medical devices-part 5: Tests for in Vitro Cytotoxicity," IOS, Geneva, 2009.
[62] T. Jurca, et al., A phytocomplex consisting of *Tropaeolum majus* L. and *Salvia officinalis* L. extracts alleviates the inflammatory response of dermal fibroblasts to bacterial lipopolysaccharides, Oxid. Med. Cell. Longev. 2020 (May 2020) 1–14, https://doi.org/10.1155/2020/8516153.
[63] M.A. Gómez-Hernández, et al., Photoprotective activity of Buddleja cordata cell culture methanolic extract on UVB-irradiated 3T3-Swiss albino fibroblasts, Plants 10 (2) (Jan. 2021) 266, https://doi.org/10.3390/plants10020266.
[64] L.A. Can-Herrera, A.I. Oliva, M.A.A. Dzul-Cervantes, O.F. Pacheco-Salazar, J. M. Cervantes-Uc, Morphological and mechanical properties of electrospun polycaprolactone scaffolds: effect of applied voltage, Polymers 13 (4) (Feb. 2021) 662, https://doi.org/10.3390/polym13040662.
[65] M. Putti, M. Simonet, R. Solberg, G.W.M. Peters, Electrospinning poly (ε-caprolactone) under controlled environmental conditions: influence on fiber morphology and orientation, Polymer (Guildf.) 63 (Apr. 2015) 189–195, https://doi.org/10.1016/j.polymer.2015.03.006.
[66] A. Radisavljevic, D.B. Stojanovic, M. Petrovic, V. Radojevic, P. Uskokovic, M. Rajilic-Stojanovic, Electrospun polycaprolactone nanofibers functionalized with Achillea millefolium extract yield biomaterial with antibacterial, antioxidant and improved mechanical properties, J. Biomed. Mater. Res. 111 (7) (Jul. 2023) 962–974, https://doi.org/10.1002/jbm.a.37481.
[67] M.J. Mochane, T.S. Motsoeneng, E.R. Sadiku, T.C. Mokhena, J.S. Sefadi, Morphology and properties of electrospun PCL and its composites for medical applications: a mini review, Appl. Sci. 9 (11) (May 2019) 2205, https://doi.org/10.3390/app9112205.
[68] W.J. Al-Kaabi, et al., Development of Inula graveolens (L.) plant extract Electrospun/Polycaprolactone nanofibers: a novel material for biomedical application, Appl. Sci. 11 (2) (Jan. 2021) 828, https://doi.org/10.3390/app11020828.
[69] D. Cicėnas, A. Šešok, Influence of different solvents on the mechanical properties of electrospun scaffolds, Materials 18 (2) (Jan. 2025) 355, https://doi.org/10.3390/ma18020355.
[70] P. Piyasin, R. Yensano, S. Pinitsoontorn, Size-Controllable melt-electrospun polycaprolactone (PCL) fibers with a sodium chloride additive, Polymers 11 (11) (Oct. 2019) 1768, https://doi.org/10.3390/polym11111768.
[71] M. Zahiri, et al., Encapsulation of curcumin loaded chitosan nanoparticle within poly (ε-caprolactone) and gelatin fiber mat for wound healing and layered dermal reconstitution, Int. J. Biol. Macromol. 153 (Jun. 2020) 1241–1250, https://doi.org/10.1016/j.ijbiomac.2019.10.255.
[72] D.A. Pompa-Monroy, et al., Bacterial biofilm Formation using PCL/Curcumin electrospun fibers and its potential use for biotechnological applications, Materials 13 (23) (Dec. 2020) 5556, https://doi.org/10.3390/ma13235556.
[73] L.J. Villarreal Gómez, et al., Study of electrospun nanofibers loaded with Ru(ii) phenanthroline complexes as a potential material for use in dye-sensitized solar cells (DSSCs), RSC Adv. 13 (51) (2023) 36023–36034, https://doi.org/10.1039/D3RA07283E.
[74] M.A. Woodruff, D.W. Hutmacher, The return of a forgotten polymer—Polycaprolactone in the 21st century, Prog. Polym. Sci. 35 (10) (Oct. 2010) 1217–1256, https://doi.org/10.1016/j.progpolymsci.2010.04.002.
[75] O.L. Torres Vargas, Y.V. Galeano Loaiza, M.L. González, Effect of incorporating extracts from natural pigments in alginate/starch films, J. Mater. Res. Technol. 13 (Jul. 2021) 2239–2250, https://doi.org/10.1016/j.jmrt.2021.05.091.
[76] A.I. Ribeiro, et al., Synergistic antimicrobial activity of silver nanoparticles with an emergent class of azoimidazoles, Pharmaceutics 15 (3) (Mar. 2023) 926, https://doi.org/10.3390/pharmaceutics15030926.
[77] A.Y. Mensah, P.J. Houghton, S. Bloomfield, A. Vlietinck, D. Vanden Berghe, Known and novel terpenes from Buddleja globosa displaying selective antifungal activity against dermatophytes, J. Nat. Prod. 63 (9) (Sep. 2000) 1210–1213, https://doi.org/10.1021/np0001023.
[78] H.Y. Al Ati, A.A. El Gamal, G.A. Fawzy, Chemical composition, in vitro antimicrobial and cytotoxic activities of Buddleja polystachya essential oils, Journal of Essential Oil Bearing Plants 17 (6) (Nov. 2014) 1112–1119, https://doi.org/10.1080/0972060X.2014.1001133.
[79] S.C. Pendota, M.A. Aderogba, A.R. Ndhlala, J. Van Staden, Antimicrobial and acetylcholinesterase inhibitory activities of Buddleja salviifolia (L.) Lam. leaf extracts and isolated compounds, J. Ethnopharmacol. 148 (2) (Jul. 2013) 515–520, https://doi.org/10.1016/j.jep.2013.04.047.
[80] J. Anand, N. Rai, Anticandidal synergistic activity of green tea catechins, antimycotics and copper sulphate as a mean of combinational drug therapy against candidiasis, J. Mycol. Med. 27 (1) (Mar. 2017) 33–45, https://doi.org/10.1016/j.mycmed.2016.08.004.
[81] Y. Ning, J. Ling, C.D. Wu, Synergistic effects of tea catechin epigallocatechin gallate and antimycotics against oral Candida species, Arch. Oral Biol. 60 (10) (Oct. 2015) 1565–1570, https://doi.org/10.1016/j.archoralbio.2015.07.001.
[82] A. Dart, et al., Highly active nisin coated polycaprolactone electrospun fibers against both Staphylococcus aureus and Pseudomonas aeruginosa, Biomater. Adv. 154 (Nov. 2023) 213641, https://doi.org/10.1016/j.bioadv.2023.213641.
[83] A.R.M. Ribeiro, et al., Sodium alginate-based multifunctional sandwich-like system for treating wound infections, Biomater. Adv. 162 (Sep. 2024) 213931, https://doi.org/10.1016/j.bioadv.2024.213931.
[84] S. Chaiarwut, P. Ekabutr, P. Chuysinuan, T. Chanamuangkon, P. Supaphol, Surface immobilization of PCL electrospun nanofibers with pexiganan for wound dressing, J. Polym. Res. 28 (9) (Sep. 2021) 344, https://doi.org/10.1007/s10965-021-02669-w.
[85] S. Raghunathan, et al., Synthesis of biocomposites from microalgal peptide incorporated polycaprolactone/κ- carrageenan nanofibers and their antibacterial and wound healing property, Int J Pharm 655 (Apr. 2024) 124052, https://doi.org/10.1016/j.ijpharm.2024.124052.
[86] A. Radisavljevic, et al., Cefazolin-loaded polycaprolactone fibers produced via different electrospinning methods: characterization, drug release and antibacterial effect, Eur. J. Pharmaceut. Sci. 124 (Nov. 2018) 26–36, https://doi.org/10.1016/j.ejps.2018.08.023.
[87] R. Ramalingam, et al., Poly-ε-Caprolactone/Gelatin hybrid electrospun composite nanofibrous mats containing ultrasound assisted herbal extract: antimicrobial and cell proliferation Study, Nanomaterials 9 (3) (Mar. 2019) 462, https://doi.org/10.3390/nano9030462.
[88] A.H. Ladio, M. Lozada, Comparison of wild edible plant diversity and foraging strategies in two aboriginal communities of northwestern Patagonia, Biodivers. Conserv. 12 (5) (May 2003) 937–951, https://doi.org/10.1023/A:1022873725432.
[89] T. Mosmann, Rapid colorimetric assay for cellular growth and survival: application to proliferation and cytotoxicity assays, J. Immunol. Methods 65 (1–2) (Dec. 1983) 55–63, https://doi.org/10.1016/0022-1759(83)90303-4.
[90] L. Kooshki, S.N. Zarneshan, S. Fakhri, S.Z. Moradi, J. Echeverria, The pivotal role of JAK/STAT and IRS/PI3K signaling pathways in neurodegenerative diseases: mechanistic approaches to polyphenols and alkaloids, Phytomedicine 112 (Apr. 2023) 154686, https://doi.org/10.1016/j.phymed.2023.154686.
[91] M. Mirza-Aghazadeh-Attari, et al., Targeting PI3K/Akt/mTOR signaling pathway by polyphenols: implication for cancer therapy, Life Sci. 255 (Aug. 2020) 117481, https://doi.org/10.1016/j.lfs.2020.117481.
[92] M. Nomura, et al., Inhibitory mechanisms of tea polyphenols on the ultraviolet B-activated phosphatidylinositol 3-Kinase-dependent pathway, J. Biol. Chem. 276 (49) (Dec. 2001) 46624–46631, https://doi.org/10.1074/jbc.M107897200.
[93] A.A. Koupai, et al., Vanillin and IGF1-loaded dual-layer multifunctional wound dressing with micro-nanofibrous structure for full-thickness wound healing

acceleration, Int J Pharm 671 (Feb. 2025) 125231, https://doi.org/10.1016/j.ijpharm.2025.125231.

[94] B.T. Al-Sudani, et al., Highly porous 3D printed scaffold incorporated with graphene oxide-merwinite and coated with IGF1 loaded nanofibers for calvarial defect repair, J. Polym. Environ. 32 (10) (Oct. 2024) 5330–5343, https://doi.org/10.1007/s10924-024-03324-3.

[95] Y. Dai, D. Sun, D. O'Rourke, S. Velusamy, S. Sundaram, M. Edirisinghe, Harnessing cow manure waste for nanocellulose extraction and sustainable small-structure manufacturing, J. Clean. Prod. 509 (Jun. 2025) 145530, https://doi.org/10.1016/j.jclepro.2025.145530.